South African Inflation Modelling Under the HJM Framework

Massimo Rizzo

A dissertation submitted to the Faculty of Commerce, University of Cape Town, in partial fulfilment of the requirements for the degree of Master of Philosophy.

September 11, 2022

MPhil in Mathematical Finance,
University of Cape Town.

Declaration

I declare that this dissertation is my own, unaided work. It is being submitted for the Degree of Master of Philosophy at the University of Cape Town. It has not been submitted before for any degree or examination in any other University.

Signed by candidate

September 11, 2022

Abstract

Inflation modelling is typically done following an econometric approach, however this results in models being constructed that are not consistent with the observable bond market and as such they cannot be used in hedging market instruments or in pricing inflation-linked derivatives. Jarrow and Yildirim (2003) were one of the first to propose a framework under which nominal and real forward rates and an inflation index could be jointly modelled in a consistent manner, based on the Heath-Jarrow-Morton (HJM) framework as first developed by Heath *et al.* (1992). They showed that under this framework it is possible to recover observed nominal and inflation-linked bond prices, hedge these instruments, and price related inflation-linked derivatives. A shortfall of this framework however, as critiqued by Mercurio (2005) and Belgrade *et al.* (2004), is that it depends entirely on non-observable parameters. As such, estimating the parameters of a model constructed under this framework is non-trivial. This dissertation applies the approach detailed by Jarrow and Yildirim (2003) to construct a model that fits the South African context, and makes use of the Kalman filter, as originally documented by Kalman (1960), to overcome the issues that arise in parameter estimation. Using the model constructed, forecasts of future inflation in South Africa are produced.

Acknowledgements

I would like to extend my sincerest thanks to my supervisor, Obeid Mahomed, for his invaluable insight and guidance, and to my family and close friends for their continual support and encouragement.

Contents

List of Figures

List of Tables

Chapter 1

Introduction

Inflation is the term given by economists to the steady increase in overall price levels in an economy over time, and as such it is an important factor to take into account when pricing long-term instruments. As specified by Raffaelli (2007), in South Africa inflation is measured by the South African Consumer Price Index (henceforth to be referred to as the CPI), defined simply as a weighted average of a collection of typical consumer goods and services. Inflation plays a core role in the investment performance of both nominal and inflation-linked bonds, and in the inflation-derivative market.

When modelling inflation, the typical approach is to employ an econometric model which forecasts the inflation rate based on a time series of observed data. These models function by relating inflation to various observable macroeconomic indicators. However, as described by Belgrade *et al.* (2004), these models are ineffective when used for hedging or derivative pricing mainly because they do not include the relationships observed between various traded instruments in their specification, and as such the model will not be consistent with observed market prices (or in other words, these models will not be arbitrage-free).

Referring to Dam *et al.* (2020) for a chronology of inflation-linked derivatives pricing, Jarrow and Yildirim (2003) were one of the first to suggest a framework which could be used to price and hedge both nominal and inflation-linked US Treasury bonds, as well as other inflation-linked derivatives. They did this by exploiting the HJM foreign currency analogy developed by Jarrow and Turnbull (1998); treating the inflation rate as an exchange rate between nominal dollars and real dollars, where the former is treated as a domestic currency and the latter a foreign currency.[1] The framework considers the relationship between instantaneous nominal and real forward rates, and an inflation index (which in our case, will be the CPI). Under this framework, they go on to specify a deterministic volatility structure which leads to the construction of a three-factor model where the modelled

[1] Here, "HJM" refers to the Heath-Jarrow-Morton framework developed by Heath *et al.* (1992).

nominal and real forward rates follow extended-Vasiček-style dynamics. Jarrow and Yildirim (2003) apply the resultant model to US Treasury inflation-protected securities, and are able to recover the prices of these instruments observed in the market. They also demonstrate the hedging ability of the model, and price a theoretical call option on the inflation index to show that it is possible to price such derivatives using the model. However, as criticised by authors Belgrade *et al.* (2004) and Mercurio (2005), the model constructed makes use of parameters that are not readily observable in the market which means that they have to be estimated using historical (or longitudinal) data. As both authors point out, this is a non-trivial exercise.

To address this, Mercurio (2005) built on the work developed by Jarrow and Yildirim (2003) and proposed two market models that could then be used for the same applications as the model developed under Jarrow and Yildirim (2003) but without having the same parameter estimation difficulties, since these market models allow for immediate calibration to observed bond market data. In the first market model, Mercurio (2005) changes the specification of the model from modelling forward rates in an HJM setting to one where the nominal and real forward rates are modelled under a lognormal LIBOR market model. The second involves an approximation to the first model to aid in numerical computation. Mercurio (2005) goes on to compare the performance of the estimated Jarrow and Yildirim (2003) model to the two proposed market models, once both have been estimated and calibrated to observed market data, in pricing year-on-year inflation-indexed swaps and zero-strike floors. It is found that all three models perform similarly when pricing the year-on-year inflation-indexed swaps, but not in pricing out-of-the-money derivatives like zero-strike floors.

At the same time as Mercurio (2005), Belgrade *et al.* (2004) also published a paper which aimed to address the shortcomings of the framework developed by Jarrow and Yildirim (2003), and derived a market model that is equivalent to the second market model proposed by Mercurio (2005). Due to this equivalence, their findings were similar.

Lastly, Mercurio and Moreni (2005) built on the work done by Mercurio (2005) and Belgrade *et al.* (2004) to provide an extension for stochastic volatility to their equivalent models, mainly to aid in the pricing of caplets and floorlets.

In this dissertation, we aim to build a model under the Jarrow and Yildirim (2003) framework that can be used to simulate both nominal and inflation-linked bond prices that are consistent with what is observed in the South African bond market. This will first involve the estimation of the model parameters using longitudinal and cross-sectional South African bond data, after which we will outline an

extension to allow for the exact calibration of the model to both nominal and real observed zero-coupon bond prices. Lastly, we use both the estimated model and the calibrated model to produce two forecasts of future inflation in South Africa.

In Chapter 2 we present the framework as proposed by Jarrow and Yildirim (2003), adjusted to fit our South African context. We then make specific modelling choices to allow for the construction of a Vasiček-style model under the framework, moving from working in terms of instantaneous forward rates to an equivalent representation where we work in terms of instantaneous short rates. We then provide a set of stochastic differential equations that fully define the dynamics of the nominal short rate, the real short rate and the CPI within the model. In Chapter 3 we propose a method to use in simulating the dynamics developed in Chapter 2, and demonstrate the simulation ability of the model. Chapter 4 deals with the estimation and calibration of the model, and involves the description and implementation of the Kalman filter, pioneered by Kalman (1960), to address the concerns of Mercurio (2005) and Belgrade *et al.* (2004) about the unobservable model parameters. We employ the Kalman filter algorithm on the simulated data created in Chapter 3 to demonstrate its ability to correctly estimate the underlying parameters, after which we then apply the Kalman filter to South African bond market data to estimate the model and produce a forecast for future inflation in South Africa. In the final section of Chapter 4 we cover the method used for exactly calibrating the model to observable bond market data, and use this calibrated model to again forecast future inflation. Chapter 5 then concludes the paper.

Chapter 2

Development of the Model

In this chapter we begin by presenting the framework as developed by Jarrow and Yildirim (2003), and adjusting it to fit the South African context. We then specify deterministic volatility functions for the nominal and real instantaneous forward rates that allow us to equivalently represent the nominal and real processes in terms of short rates, and in turn model these under the Vasiček model as developed by Vasiček (1977). Lastly, we provide two equivalent representations of the constructed model that will aid us in the simulation and estimation procedures to be covered in Chapters 3 and 4.

2.1 The Jarrow and Yildirim Framework

Before presenting the framework itself, we begin with an introductory exposition where we cover the assumptions concerning the modelled market and all of the most critical notation to make the derivations that follow more interpretable.

2.1.1 An Introduction to the Framework

Jarrow and Yildirim (2003) consider a continuous trading economy with finite time horizon $[0, \tau]$. It is assumed that the modelled market is friction-less (i.e., there are no transaction costs, no taxes, and no profit margins), that the market is completely divisible (i.e., there are no restrictions on trades: assets can be traded in any amounts and short sales are permitted), there is no default risk, and there are no arbitrage opportunities. The uncertainty of the economy is characterised by the probability space $(\Omega, \mathcal{F}, \mathbb{P})$, where Ω is the state space, $\mathcal{F}$ is a σ-algebra on Ω and represents the set of all decidable events, and $\mathbb{P}$ is the real world probability measure on $(\Omega, \mathcal{F})$. $\{\mathcal{F}_t : t \in [0, \tau]\}$ is defined as the standard filtration generated by the three-dimensional correlated standard $\mathbb{P}$-Brownian motion $\{W_n^{\mathbb{P}}(t), W_r^{\mathbb{P}}(t), W_I^{\mathbb{P}}(t) : t \in [0, \tau]\}$. The correlations between each of these Brownian motions are specified

as follows:

$$dW_n^{\mathbb{P}}(t)\,dW_r^{\mathbb{P}}(t) = \rho_{nr}\,dt, \quad dW_n^{\mathbb{P}}(t)\,dW_I^{\mathbb{P}}(t) = \rho_{nI}\,dt, \quad dW_r^{\mathbb{P}}(t)\,dW_I^{\mathbb{P}}(t) = \rho_{rI}\,dt.$$

In order to ease the exposition that follows, all of the most critical notation is first presented here:

$P_n(t,T)$ The time t price of a nominal zero-coupon bond maturing at time $T \in [t,\tau]$, with a maturity value of 1 nominal unit (i.e., R1).

$I(t)$ The time t South African CPI (with a time lag of four months – in South Africa, to allow time for the collection of the typical consumer basket's constituents, the CPI is published with a four month lag. This allows for inflation-linked payments to be made without having to wait for the current month's CPI value to be published). For all of the mathematical derivations to follow, we make the assumption that $I(0) = 1$ (i.e., that the CPI at the issue date of all considered inflation-linked bonds is 1).

$P_r(t,T)$ The time t price of a real zero-coupon bond maturing at time T in real units (or, in terms of the foreign exchange analogy, units of real currency), with a maturity value of 1 real unit.

$P_{ILB}(t,T)$ The time t price of an inflation-linked zero-coupon bond maturing at time T, with a maturity value of $\frac{I(T)}{I(0)} = I(T)$ (recall that we assume all inflation-linked bonds are issued at time 0, and that $I(0) = 1$). Thus we can define the price of an inflation-linked zero-coupon bond as:

$$P_{ILB}(t,T) = I(t)P_r(t,T).$$

$f_x(t,T)$ The time t instantaneous forward rate for date T where $x \in \{r,n\}$ (corresponding to "nominal" and "real" respectively). We can thus write the zero-coupon bond price in terms of instantaneous forward rates for $x \in \{r,n\}$ as:

$$P_x(t,T) = e^{-\int_t^T f_x(t,s)\,ds}.$$

$r_x(t)$ The time t instantaneous short rate, such that $r_x(t) = f_x(t,t)$, where $x \in \{r,n\}$.

$B_x(t)$ The time t money market account value for $x \in \{r,n\}$, which we can write in terms of instantaneous short rates as:

$$B_x(t) = e^{\int_0^t r_x(s)\,ds}.$$

2.1.2 Framework Dynamics Under the Real-World Measure

We can now begin our presentation of the Jarrow and Yildirim framework. In the same way as Jarrow and Yildirim (2003), we first define the nominal instantaneous forward rate dynamics, real instantaneous forward rate dynamics and the CPI dynamics under the real-world measure $\mathbb{P}$.

Nominal Instantaneous Forward Rate Dynamics

Given the initial forward rate curve $f_n(0,T)$ for $T \in [0,\tau]$, it is assumed that the nominal instantaneous forward rate has the following $\mathbb{P}$-dynamics:

$$df_n(t,T) = \alpha_n(t,T)\,dt + \sigma_n(t,T)\,dW_n^{\mathbb{P}}(t), \tag{2.1}$$

where $\alpha_n(t,T)$ and $\sigma_n(t,T)$ are both deterministic functions of time subject to a set of technical smoothness and boundedness conditions, which are covered in detail in Jarrow and Yildirim (2003). Because of the deterministic volatility term, the nominal term structure of interest rates generates a normally-distributed economy (which is appealing due to its computational simplicity, however it must be noted that this allows for negative nominal interest rates).

Real Instantaneous Forward Rate Dynamics

Given the initial forward rate curve $f_r(0,T)$ for $T \in [0,\tau]$, it is similarly assumed that the real instantaneous forward rate has the following $\mathbb{P}$-dynamics:

$$df_r(t,T) = \alpha_r(t,T)\,dt + \sigma_r(t,T)\,dW_r^{\mathbb{P}}(t), \tag{2.2}$$

where $\alpha_r(t,T)$ and $\sigma_r(t,T)$ are subject to the same technical smoothness and boundedness conditions mentioned above.

Consumer Price Index Dynamics

It is assumed that the CPI has the following $\mathbb{P}$-dynamics:

$$\frac{dI(t)}{I(t)} = \mu_I(t)\,dt + \sigma_I(t)\,dW_I^{\mathbb{P}}(t), \tag{2.3}$$

where $\mu_I(t)$ is a stochastic function (which we will show is dependant on the instantaneous short rates $r_n(t)$ and $r_r(t)$) and $\sigma_I(t)$ is a deterministic function of time. Both are subject to a set of technical smoothness and boundedness conditions similar to the forward rate dynamics defined above, and are again covered in detail in Jarrow and Yildirim (2003). Due to the deterministic volatility term, the natural logarithm of $I(t)$ will be normally distributed, which relates conveniently to the normally-distributed nominal and real instantaneous forward rates defined above.

2.1.3 Arbitrage-Free Drift Conditions

Now that we have defined the framework dynamics under the real-world measure $\mathbb{P}$, we can derive expressions for the drift functions $\alpha_n(t,T)$, $\alpha_r(t,T)$ and $\mu_I(t)$ by moving to an equivalent representation under the risk-neutral measure $\mathbb{Q}$. By the second fundamental theorem of asset pricing as described in Björk (2009), the above real-world dynamics are arbitrage-free, and the modelled market is complete, if and only if there exists a unique and equivalent probability measure $\mathbb{Q}$ such that the following are all $\mathbb{Q}$-martingales (i.e., have driftless stochastic differential equations):

$$\frac{P_n(t,T)}{B_n(t)}, \qquad \frac{I(t)P_r(t,T)}{B_n(t)}, \qquad \frac{I(t)B_r(t)}{B_n(t)}.$$

Given that $\{W_n^{\mathbb{P}}(t), W_r^{\mathbb{P}}(t), W_I^{\mathbb{P}}(t) : t \in [0,\tau]\}$ is a standard correlated $\mathbb{P}$-Brownian motion and assuming that $\mathbb{Q}$ exists and is equivalent to $\mathbb{P}$, then by Girsanov's theorem as described in Björk (2009) there exist the processes $\{\lambda_n(t), \lambda_r(t), \lambda_I(t) : t \in [0,\tau]\}$ such that

$$dW_x^{\mathbb{Q}}(t) = dW_x^{\mathbb{P}}(t) - \lambda_x(t)\,dt, \qquad \text{for } x \in \{n, r, I\}, \tag{2.4}$$

are standard correlated $\mathbb{Q}$-Brownian motions. The processes $\{\lambda_n(t), \lambda_r(t), \lambda_I(t) : t \in [0,\tau]\}$ are in fact the market prices of risk for the three-factor economy constructed. Note that the correlations of the $\mathbb{P}$-Brownian motions are preserved under a change of measure, i.e.,

$$dW_n^{\mathbb{Q}}(t)\,dW_r^{\mathbb{Q}}(t) = \rho_{nr}\,dt, \quad dW_n^{\mathbb{Q}}(t)\,dW_I^{\mathbb{Q}}(t) = \rho_{nI}\,dt, \quad dW_r^{\mathbb{Q}}(t)\,dW_I^{\mathbb{Q}}(t) = \rho_{rI}\,dt.$$

Now, we can show that $\frac{P_n(t,T)}{B_n(t)}$, $\frac{I(t)P_r(t,T)}{B_n(t)}$, and $\frac{I(t)B_r(t)}{B_n(t)}$ are $\mathbb{Q}$-martingales if and only if the following drift conditions hold:

$$\alpha_n(t,T) = \sigma_n(t,T)\left(\int_t^T \sigma_n(t,s)\,ds - \lambda_n(t)\right), \tag{2.5}$$

$$\alpha_r(t,T) = \sigma_r(t,T)\left(\int_t^T \sigma_r(t,s)\,ds - \sigma_I(t)\rho_{rI} - \lambda_r(t)\right), \tag{2.6}$$

$$\mu_I(t) = r_n(t) - r_r(t) - \sigma_I(t)\lambda_I(t). \tag{2.7}$$

The proofs of the above conditions have been included in Appendix A.1. Notice how equation (2.5) is the arbitrage-free forward rate drift restriction as in the original HJM framework (see Heath *et al.* (1992)), equation (2.6) is the analogous arbitrage-free forward rate drift restriction for the real forward rates (take note that the volatility of inflation and its correlation to the real forward rate appears here), and equation (2.7) is related to the Fisher equation (expected inflation $\approx$ nominal

interest rates − real interest rates). This can be seen more clearly when in the next section, we show that under $\mathbb{Q}$ the drift component of $\frac{dI(t)}{I(t)}$ (i.e., "expected inflation") is $[r_n(t) - r_r(t)]\,dt$ (i.e., "nominal interest rates − real interest rates").

2.1.4 Framework Dynamics Under the Risk-Neutral Measure

We are now able to represent our instantaneous forward rate and CPI dynamics under the risk-neutral measure $\mathbb{Q}$. Utilising the Girsanov transformation described in equation (2.4), and substituting the arbitrage-free drift conditions (2.5), (2.6) and (2.7) into the real-world dynamics (2.1), (2.2) and (2.3) respectively, we can easily derive the following framework $\mathbb{Q}$-dynamics:

$$df_n(t,T) = \sigma_n(t,T)\left[\int_t^T \sigma_n(t,s)\,ds\right]\,dt + \sigma_n(t,T)\,dW_n^{\mathbb{Q}}(t), \tag{2.8}$$

$$df_r(t,T) = \sigma_r(t,T)\left[\int_t^T \sigma_r(t,s)\,ds - \rho_{rI}\sigma_I(t)\right]\,dt + \sigma_r(t,T)\,dW_r^{\mathbb{Q}}(t), \tag{2.9}$$

$$\frac{dI(t)}{I(t)} = [r_n(t) - r_r(t)]\;dt + \sigma_I(t)\,dW_I^{\mathbb{Q}}(t).$$

For completeness, we also present the $\mathbb{Q}$-dynamics for the zero-coupon bond prices $P_n(t,T)$, $P_r(t,T)$ and $P_{ILB}(t,T)$ as derived by Jarrow and Yildirim (2003):

$$\frac{dP_n(t,T)}{P_n(t,T)} = r_n(t)\,dt - \int_t^T \sigma_n(t,s)\,ds\,dW_n^{\mathbb{Q}}(t),$$

$$\frac{dP_r(t,T)}{P_r(t,T)} = \left[r_r(t) - \rho_{rI}\sigma_I(t)\int_t^T \sigma_r(t,s)\,ds\right]\,dt - \int_t^T \sigma_r(t,s)\,ds\,dW_r^{\mathbb{Q}}(t),$$

$$\frac{dP_{ILB}(t,T)}{P_{ILB}(t,T)} = r_n(t)\,dt + \sigma_I(t)\,dW_I^{\mathbb{Q}}(t) - \int_t^T \sigma_r(t,s)\,ds\,dW_r^{\mathbb{Q}}(t).$$

We will however not be making use of these bond price dynamics, and as such their proofs have been omitted.

2.2 The Short Rate Model

In this section, we make specific choices for the volatility functions $\sigma_n(t,T)$, $\sigma_r(t,T)$ and $\sigma_I(t)$ that allow us to construct a short rate model under the Jarrow and Yildirim (2003) framework. We also present both the risk-neutral and real-world dynamics for this model.

2.2.1 Specification of Volatility Functions

We specify the following forward rate and inflation volatility functions:

$$\sigma_n(t,T) := \sigma_n e^{-a_n(T-t)}, \tag{2.10}$$
$$\sigma_r(t,T) := \sigma_r e^{-a_r(T-t)}, \tag{2.11}$$
$$\sigma_I(t) := \sigma_I, \tag{2.12}$$

where σ_n, σ_r, σ_I, a_n, a_r are all constants. Under this specification we move from the nominal and real instantaneous forward rate models to an equivalent representation in terms of nominal and real instantaneous short rates. Following Mercurio (2005) we arrive at the following Hull-White Extended Vasiček $\mathbb{Q}$-dynamics for the nominal and real short rate (note that the CPI process remains unchanged):

$$dr_n(t) = [b_n(t) - a_n r_n(t)]\ dt + \sigma_n\, dW_n^{\mathbb{Q}}(t), \tag{2.13}$$
$$dr_r(t) = [b_r(t) - \rho_{rI}\sigma_I\sigma_r - a_r r_r(t)]\ dt + \sigma_r\, dW_r^{\mathbb{Q}}(t), \tag{2.14}$$
$$\frac{dI(t)}{I(t)} = [r_n(t) - r_r(t)]\ dt + \sigma_I\, dW_I^{\mathbb{Q}}(t),$$

where $b_n(t)$ and $b_r(t)$ are deterministic functions used to exactly fit the initial term structure of nominal and real forward rates, i.e.,

$$b_x(t) = \frac{\partial f_x(0,t)}{\partial T} + a_x f_x(0,t) + \frac{\sigma_x^2}{2a_x}\left(1 - e^{-2a_x t}\right), \qquad x \in \{n, r\},$$

where $\frac{\partial f_x}{\partial T}$ denotes the partial derivative of f_x with respect to its second argument. The proofs of equations (2.13) and (2.14) have been included in Appendix A.2.

2.2.2 Risk-Neutral Dynamics

Since our aim initially is to estimate the model under the real-world measure $\mathbb{P}$ and not to calibrate under the risk-neutral measure $\mathbb{Q}$, we will be specifying that $b_n(t)$ and $b_r(t)$ are in fact constant parameters (i.e., $b_n(t) = b_n$, and $b_r(t) = b_r$). This is a necessary specification as the estimation procedure we will be employing requires the nominal and real short-rate dynamics to be time-homogeneous. Thus we arrive at the following three-factor model under $\mathbb{Q}$:

$$dr_n(t) = [b_n - a_n r_n(t)]\ dt + \sigma_n\, dW_n^{\mathbb{Q}}(t), \tag{2.15}$$
$$dr_r(t) = [b_r - \rho_{rI}\sigma_I\sigma_r - a_r r_r(t)]\ dt + \sigma_r\, dW_r^{\mathbb{Q}}(t), \tag{2.16}$$
$$\frac{dI(t)}{I(t)} = [r_n(t) - r_r(t)]\ dt + \sigma_I\, dW_I^{\mathbb{Q}}(t). \tag{2.17}$$

2.2.3 Real-World Dynamics

To move back to the real-world measure $\mathbb{P}$, we use equation (2.4) to incorporate a market price of risk parameter in the drift of the two instantaneous short rate processes and the CPI process. We will be assuming a constant market price of risk for all three processes, i.e., $\lambda_n(t) = \lambda_n$, $\lambda_r(t) = \lambda_r$, and $\lambda_I(t) = \lambda_I$, and so equation (2.4) becomes:

$$dW_x^{\mathbb{Q}}(t) = dW_x^{\mathbb{P}}(t) - \lambda_x \, dt, \qquad \text{for } x \in \{n, r, I\}.$$

The $\mathbb{P}$-dynamics of the three-factor model can then be specified as follows:

$$dr_n(t) = [b_n - \sigma_n \lambda_n - a_n r_n(t)] \; dt + \sigma_n \, dW_n^{\mathbb{P}}(t), \tag{2.18}$$

$$dr_r(t) = [b_r - \rho_{rI}\sigma_I\sigma_r - \sigma_r\lambda_r - a_r r_r(t)] \; dt + \sigma_r \, dW_r^{\mathbb{P}}(t), \tag{2.19}$$

$$\frac{dI(t)}{I(t)} = [r_n(t) - r_r(t) - \sigma_I\lambda_I] \; dt + \sigma_I \, dW_I^{\mathbb{P}}(t). \tag{2.20}$$

In both the risk-neutral and the real-world representation, $r_n(t)$ and $r_r(t)$ are modelled under the Vasiček short rate model (see Vasiček (1977)). This choice has been made specifically since the Vasiček model is time-homogeneous which is a property that is required by the estimation procedure we will be employing. Lastly, it must be noted that modelling short rates under the Vasiček model allows for negative short rates. If it were a requirement that short rates remain positive, it would be worthwhile to instead consider the CIR model for short rates (see Brigo and Mercurio (2006)).

2.3 An Equivalent Representation of the Short Rate Model

In this section, we present an equivalent representation of the model constructed in the previous section, where we move from working with respect to the three-dimensional correlated standard $\mathbb{Q}$-Brownian motion $\{W_n^{\mathbb{Q}}(t), W_r^{\mathbb{Q}}(t), W_I^{\mathbb{Q}}(t) : t \in [0, \tau]\}$ to instead the three-dimensional independent standard $\mathbb{Q}$-Brownian motion $\{\tilde{W}_1^{\mathbb{Q}}(t), \tilde{W}_2^{\mathbb{Q}}(t), \tilde{W}_3^{\mathbb{Q}}(t) : t \in [0, \tau]\}$. The reason for this is only to make simulation computationally simpler, and it is important to note that this change has no effect on the correlations between $r_n(t)$, $r_r(t)$ and $I(t)$ that are such an intrinsic part of the developed three-factor model. We would like to emphasise the fact that we will still be using the original representation of the model (i.e., with respect to the correlated Brownian motions) for estimating the model's parameters (as there will then be fewer parameters that are required to be estimated).

2.3.1 Risk-Neutral Dynamics

Representing equations (2.15), (2.16) and (2.17) with respect to the three-dimensional independent standard $\mathbb{Q}$-Brownian motion $\{\tilde{W}_1^{\mathbb{Q}}(t), \tilde{W}_2^{\mathbb{Q}}(t), \tilde{W}_3^{\mathbb{Q}}(t) : t \in [0, \tau]\}$ requires us to specify the $\mathbb{Q}$-dynamics as follows:

$$\begin{bmatrix} dr_n(t) \\ dr_r(t) \\ \frac{dI(t)}{I(t)} \end{bmatrix} = \begin{bmatrix} b_n - a_n r_n(t) \\ b_r - \rho_{rI}\sigma_I\sigma_r - a_r r_r(t) \\ r_n(t) - r_r(t) \end{bmatrix} dt + \begin{bmatrix} \tilde{\sigma}_{11} & \tilde{\sigma}_{12} & \tilde{\sigma}_{13} \\ \tilde{\sigma}_{21} & \tilde{\sigma}_{22} & \tilde{\sigma}_{23} \\ \tilde{\sigma}_{31} & \tilde{\sigma}_{32} & \tilde{\sigma}_{33} \end{bmatrix} \begin{bmatrix} d\tilde{W}_1^{\mathbb{Q}}(t) \\ d\tilde{W}_2^{\mathbb{Q}}(t) \\ d\tilde{W}_3^{\mathbb{Q}}(t) \end{bmatrix}.$$

Making the following definitions,

$$\tilde{\Sigma} := \begin{bmatrix} \tilde{\sigma}_{11} & \tilde{\sigma}_{12} & \tilde{\sigma}_{13} \\ \tilde{\sigma}_{21} & \tilde{\sigma}_{22} & \tilde{\sigma}_{23} \\ \tilde{\sigma}_{31} & \tilde{\sigma}_{32} & \tilde{\sigma}_{33} \end{bmatrix}, \qquad d\tilde{W}^{\mathbb{Q}}(t) := \begin{bmatrix} d\tilde{W}_1^{\mathbb{Q}}(t) \\ d\tilde{W}_2^{\mathbb{Q}}(t) \\ d\tilde{W}_3^{\mathbb{Q}}(t) \end{bmatrix},$$

allows us to neatly write:

$$\begin{aligned} dr_n(t) &= [b_n - a_n r_n(t)]\, dt + \tilde{\Sigma}_1\, d\tilde{W}^{\mathbb{Q}}(t), \\ dr_r(t) &= \left[b_r - \tilde{\Sigma}_2 \cdot \tilde{\Sigma}_3 - a_r r_r(t)\right] dt + \tilde{\Sigma}_2\, d\tilde{W}^{\mathbb{Q}}(t), \\ \frac{dI(t)}{I(t)} &= [r_n(t) - r_r(t)]\, dt + \tilde{\Sigma}_3\, d\tilde{W}^{\mathbb{Q}}(t), \end{aligned}$$

where $\tilde{\Sigma}_1$ is defined as the first row of $\tilde{\Sigma}$, $\tilde{\Sigma}_2$ is the second row of $\tilde{\Sigma}$ and $\tilde{\Sigma}_3$ is the third row of $\tilde{\Sigma}$ (note also that we have replaced $\rho_{rI}\sigma_I\sigma_r$ with $\tilde{\Sigma}_2 \cdot \tilde{\Sigma}_3$ in accordance with the volatility and correlation conditions defined below). For this representation to hold true, we have the following volatility conditions:

$$\sigma_n = \|\tilde{\Sigma}_1\|, \tag{2.21}$$

$$\sigma_r = \|\tilde{\Sigma}_2\|, \tag{2.22}$$

$$\sigma_I = \|\tilde{\Sigma}_3\|, \tag{2.23}$$

and the following correlation conditions:

$$\rho_{nr} = \frac{\tilde{\Sigma}_1 \cdot \tilde{\Sigma}_2}{\|\tilde{\Sigma}_1\| \times \|\tilde{\Sigma}_2\|}, \tag{2.24}$$

$$\rho_{nI} = \frac{\tilde{\Sigma}_1 \cdot \tilde{\Sigma}_3}{\|\tilde{\Sigma}_1\| \times \|\tilde{\Sigma}_3\|}, \tag{2.25}$$

$$\rho_{rI} = \frac{\tilde{\Sigma}_2 \cdot \tilde{\Sigma}_3}{\|\tilde{\Sigma}_2\| \times \|\tilde{\Sigma}_3\|}. \tag{2.26}$$

The proofs for all of the above are included in Appendix A.3. As long as the above equations are enforced, there is no difference between the model with respect to the correlated $\mathbb{Q}$-Brownian motions or the independent $\mathbb{Q}$-Brownian motions, except for the fact that it will be simpler to simulate under the latter representation.

2.3.2 Real-World Dynamics

In a similar manner, we can also represent the equations (2.18), (2.19) and (2.20) with respect to the three-dimensional independent standard $\mathbb{P}$-Brownian motion $\{\tilde{W}_1^{\mathbb{P}}(t), \tilde{W}_2^{\mathbb{P}}(t), \tilde{W}_3^{\mathbb{P}}(t) : t \in [0, \tau]\}$. First, let us define:

$$\tilde{\Lambda} := \begin{bmatrix} \tilde{\lambda}_1 \\ \tilde{\lambda}_2 \\ \tilde{\lambda}_3 \end{bmatrix},$$

such that we can rewrite equation (2.4) as:

$$d\tilde{W}^{\mathbb{Q}}(t) = d\tilde{W}^{\mathbb{P}}(t) - \tilde{\Lambda}\, dt.$$

In this way, we can then write the model's $\mathbb{P}$-dynamics with respect the the independent Brownian motions as:

$$dr_n(t) = \left[b_n - \tilde{\Sigma}_1\tilde{\Lambda} - a_n r_n(t)\right]\, dt + \tilde{\Sigma}_1\, d\tilde{W}^{\mathbb{P}}(t), \tag{2.27}$$

$$dr_r(t) = \left[b_r - \tilde{\Sigma}_2 \cdot \tilde{\Sigma}_3 - \tilde{\Sigma}_2\tilde{\Lambda} - a_r r_r(t)\right]\, dt + \tilde{\Sigma}_2\, d\tilde{W}^{\mathbb{P}}(t), \tag{2.28}$$

$$\frac{dI(t)}{I(t)} = \left[r_n(t) - r_r(t) - \tilde{\Sigma}_3\tilde{\Lambda}\right]\, dt + \tilde{\Sigma}_3\, d\tilde{W}^{\mathbb{P}}(t). \tag{2.29}$$

The same volatility and correlation conditions as defined for the risk-neutral dynamics are required to hold, as well as the following conditions to relate $\tilde{\Lambda}$ to our already established market prices of risk λ_n, λ_r, λ_I:

$$\lambda_n = \frac{\tilde{\Sigma}_1\tilde{\Lambda}}{\|\tilde{\Sigma}_1\|}, \tag{2.30}$$

$$\lambda_r = \frac{\tilde{\Sigma}_2\tilde{\Lambda}}{\|\tilde{\Sigma}_2\|}, \tag{2.31}$$

$$\lambda_I = \frac{\tilde{\Sigma}_3\tilde{\Lambda}}{\|\tilde{\Sigma}_3\|}. \tag{2.32}$$

The proofs for these equations have also been included in Appendix A.3.

Chapter 3

Simulation

In this chapter, we will discuss the methodology to be followed in simulating $r_n(t)$, $r_r(t)$ and $I(t)$ in our constructed model. We will show that once we have these simulated quantities, due to the affine nature of the derived dynamics we are easily able to calculate the zero-coupon bond prices $P_n(t,T)$ and $P_r(t,T)$.

3.1 The Vasiček Model

We begin with a brief exposition of the Vasiček model, pioneered by Vasiček (1977), in order to make the derivations that follow more succinct. Under the Vasiček model, the instantaneous short rate is described by using the following Ornstein-Uhlenbeck process:

$$dr(t) = [b - ar(t)]\ dt + \sigma\, dW^{\mathbb{Q}}(t).$$

Under this characterisation, we can rearrange the drift term $[b - ar(t)] = a[\frac{b}{a} - r(t)]$ such that we can interpret a as the rate of mean reversion and $\frac{b}{a}$ as the mean reversion level. Using Itô's lemma, Brigo and Mercurio (2006) show that the solution to this stochastic differential equation is as follows for $T > t$:

$$r(T) = e^{-a(T-t)}r(t) + \frac{b}{a}\left(1 - e^{-a(T-t)}\right) + \sigma \int_t^T e^{-a(T-s)}\, dW^{\mathbb{Q}}(s).$$

Now since the Vasiček model is an affine term structure model, by writing $P(t,T) = \mathbb{E}_{\mathbb{Q}}\left[e^{-\int_t^T r(s)\,ds}\middle|\mathcal{F}_t\right]$ and defining the following functions:

$$\begin{aligned} D(t,T) &:= \frac{1}{a}\left(1 - e^{-a(T-t)}\right), \\ C(t,T) &:= -\frac{\sigma^2 D^2(t,T)}{4a} + \frac{\big(D(t,T) - (T-t)\big)\big(ab - \frac{1}{2}\sigma^2\big)}{a^2}, \end{aligned}$$

we can follow the method used by Brigo and Mercurio (2006) to show that $P(t,T)$ takes the following form:

$$P(t,T) = e^{C(t,T) - D(t,T)r(t)}.$$

As mentioned in Chapter 2, it is important to note that the Vasiček model is time-homogeneous. This means that while the conditional distribution of $r(T)|\mathcal{F}_t$ does depend on $r(t)$ and $T-t$, it does not depend directly on t. This can intuitively be seen by the fact that functions $D(t,T)$ and $C(t,T)$ do not depend on the current time t, only the length of time to maturity $T-t$.

As shown in Chapter 2, the nominal short rate and the real short rate are both modelled under the Vasiček model, and thus we can just substitute parameters into the above specification to arrive at solutions for $r_n(t)$ and $r_r(t)$.

3.2 Simulation of the Nominal Short Rate

In deriving equations for the simulation of the nominal short rate, because we have two equivalent representations that we will be making use of (i.e., one with respect to the correlated Brownian motion $W_n^{\mathbb{P}}(t)$ and the other with respect to the independent Brownian motions $\tilde{W}^{\mathbb{P}}(t)$), we will provide derivations for both. However, as the correlated representation is not required for simulation, we do not go into as much detail as in the independent representation (however it is still important that we derive the distribution of $r_n(T)|\mathcal{F}_t$ under the correlated representation as we will be making use of these equations in Chapter 4).

3.2.1 Correlated Dynamics

Recall from equation (2.18) that the correlated $\mathbb{P}$-dynamics for the nominal short rate are as follows:

$$dr_n(t) = [b_n - \sigma_n\lambda_n - a_n r_n(t)]\ dt + \sigma_n\, dW_n^{\mathbb{P}}(t).$$

Note that under this characterisation, we can interpret a_n as the rate of mean reversion and $\frac{b_n-\sigma_n\lambda_n}{a_n}$ as the mean reversion level. Substituting parameters into the Vasiček model described in section 3.1, we arrive at the following solution for $r_n(T)$ for $T > t$:

$$\begin{aligned} r_n(T) = e^{-a_n(T-t)}r_n(t) + \frac{b_n-\sigma_n\lambda_n}{a_n}\left(1-e^{-a_n(T-t))}\right) \\ + \sigma_n\int_t^T e^{-a_n(T-s)}\, dW_n^{\mathbb{P}}(s). \end{aligned} \tag{3.1}$$

In the same manner, we can define the functions $C_n(t,T)$ and $D_n(t,T)$ as follows:

$$\begin{aligned} D_n(t,T) &:= \frac{1}{a_n}\left(1-e^{-a_n(T-t)}\right), \\ C_n(t,T) &:= -\frac{\sigma_n^2 D_n^2(t,T)}{4a_n} + \frac{\left(D_n(t,T)-(T-t)\right)\left(a_n(b_n-\sigma_n\lambda_n)-\frac{1}{2}\sigma_n^2\right)}{a_n^2}. \end{aligned}$$

Now, by the properties of an Itô integral (see Björk (2009)):

$$\int_t^T e^{-a_n(T-s)}\, dW_n^{\mathbb{P}}(s) \sim N\left(0, \int_t^T e^{-2a_n(T-s)}\, ds\right).$$

Thus we can compute the distribution of $r_n(T)|\mathcal{F}_t$ as follows:

$$r_n(T)|\mathcal{F}_t \sim N\Big(\mathbb{E}_{\mathbb{P}}\left[r_n(T)|\mathcal{F}_t\right], \mathbb{V}_{\mathbb{P}}\left[r_n(T)|\mathcal{F}_t\right]\Big),$$

where:

$$\begin{aligned}\mathbb{E}_{\mathbb{P}}\left[r_n(T)|\mathcal{F}_t\right] &= r_n(t) + \big(b_n - \sigma_n\lambda_n - a_n r_n(t)\big)D_n(t,T),\\ \mathbb{V}_{\mathbb{P}}\left[r_n(T)|\mathcal{F}_t\right] &= \frac{\sigma_n^2}{2}D_n(2t,2T).\end{aligned} \tag{3.2}$$

This distribution will be used in Chapter 4 to create the nominal transition equation for the Kalman filter.

3.2.2 Independent Dynamics

Similarly to the above correlated case, recall from equation (2.27) that the independent $\mathbb{P}$-dynamics for the nominal short rate are as follows:

$$\begin{aligned}dr_n(t) &= \left[b_n - \tilde{\Sigma}_1\tilde{\Lambda} - a_n r_n(t)\right]\, dt + \tilde{\Sigma}_1\, d\tilde{W}^{\mathbb{P}}(t)\\ &= \left[b_n - \tilde{\Sigma}_1\tilde{\Lambda} - a_n r_n(t)\right]\, dt + \tilde{\sigma}_{11}\, d\tilde{W}_1^{\mathbb{P}}(t) + \tilde{\sigma}_{12}\, d\tilde{W}_2^{\mathbb{P}}(t) + \tilde{\sigma}_{13}\, d\tilde{W}_3^{\mathbb{P}}(t).\end{aligned}$$

Now, we cannot just substitute parameters as in the correlated case, so we follow the same method as employed by Brigo and Mercurio (2006) to solve this stochastic differential equation. By Itô's lemma:

$$\begin{aligned}d\big(e^{a_n s}r_n(s)\big) &= a_n e^{a_n s} r_n(s)\, ds + e^{a_n s}\, dr_n(s)\\ &= e^{a_n s}\left[b_n - \tilde{\Sigma}_1\tilde{\Lambda}\right]\, ds\\ &\qquad + \tilde{\sigma}_{11}e^{a_n s}\, d\tilde{W}_1^{\mathbb{P}}(s) + \tilde{\sigma}_{12}e^{a_n s}\, d\tilde{W}_2^{\mathbb{P}}(s) + \tilde{\sigma}_{13}e^{a_n s}\, d\tilde{W}_3^{\mathbb{P}}(s).\end{aligned}$$

Integrating both sides from t to T:

$$\begin{aligned}e^{a_n T}r_n(T) = e^{a_n t}r_n(t) &+ \left[b_n - \tilde{\Sigma}_1\tilde{\Lambda}\right]\int_t^T e^{a_n s}\, ds\\ &+ \tilde{\sigma}_{11}\int_t^T e^{a_n s}\, d\tilde{W}_1^{\mathbb{P}}(s) + \tilde{\sigma}_{12}\int_t^T e^{a_n s}\, d\tilde{W}_2^{\mathbb{P}}(s) + \tilde{\sigma}_{13}\int_t^T e^{a_n s}\, d\tilde{W}_3^{\mathbb{P}}(s).\end{aligned}$$

Simplifying, we end up at a visually similar solution for $r_n(T)$ as in the correlated case:

$$\begin{aligned}r_n(T) = e^{a_n(T-t)}r_n(t) + \frac{b_n - \tilde{\Sigma}_1\tilde{\Lambda}}{a_n}\left(1 - e^{a_n(T-t)}\right) &+ \tilde{\sigma}_{11}\int_t^T e^{-a_n(T-s)}\, d\tilde{W}_1^{\mathbb{P}}(s)\\ &+ \tilde{\sigma}_{12}\int_t^T e^{-a_n(T-s)}\, d\tilde{W}_2^{\mathbb{P}}(s) + \tilde{\sigma}_{13}\int_t^T e^{-a_n(T-s)}\, d\tilde{W}_3^{\mathbb{P}}(s).\end{aligned}$$

Note that, by the properties of an Itô integral:

$$\int_t^T e^{-a_n(T-s)}\, d\tilde{W}_i^{\mathbb{P}}(s) \sim N\left(0, \int_t^T e^{-2a_n(T-s)}\, ds\right), \qquad \text{for } i \in \{1,2,3\}.$$

Now since, in the same way as in the correlated case:

$$\int_t^T e^{-2a_n(T-s)}\, ds = \frac{1}{2} D_n(2t, 2T),$$

we can then write the simulated value for $r_n(T)|\mathcal{F}_t$ as follows:

$$\begin{aligned} r_n(T) = r_n(t) + \big(b_n - \tilde{\Sigma}_1\tilde{\Lambda} - a_n r_n(t)\big) D_n(t,T) + \tilde{\sigma}_{11}\sqrt{\tfrac{1}{2}D_n(2t,2T)}\,\tilde{Z}_{1,t} \\ + \tilde{\sigma}_{12}\sqrt{\tfrac{1}{2}D_n(2t,2T)}\,\tilde{Z}_{2,t} + \tilde{\sigma}_{13}\sqrt{\tfrac{1}{2}D_n(2t,2T)}\,\tilde{Z}_{3,t}, \end{aligned} \tag{3.3}$$

where $\tilde{Z}_{1,t} \sim N(0,1)$, $\tilde{Z}_{2,t} \sim N(0,1)$ and $\tilde{Z}_{3,t} \sim N(0,1)$ are all independent normal variates.

3.3 Simulation of the Real Short Rate

Following the exact same methodology as in section 3.2, we will be presenting equations for simulating the real short rate under both the correlated and the independent representation.

3.3.1 Correlated Dynamics

Recall from equation (2.19) that the correlated $\mathbb{P}$-dynamics for the real short rate are as follows:

$$dr_r(t) = \left[b_r - \rho_{rI}\sigma_I\sigma_r - \sigma_r\lambda_r - a_r r_r(t)\right] dt + \sigma_r\, dW_r^{\mathbb{P}}(t).$$

Note that under this characterisation, we can interpret a_r as the rate of mean reversion and $\frac{b_r - \rho_{rI}\sigma_I\sigma_r - \sigma_r\lambda_r}{a_r}$ as the mean reversion level. Again, just substituting parameters in the Vasiček model, we arrive at the following solution for $r_r(T)$ for $T > t$:

$$\begin{aligned} r_r(T) = e^{-a_r(T-t)} r_r(t) + \frac{b_r - \rho_{rI}\sigma_I\sigma_r - \sigma_r\lambda_r}{a_r}\left(1 - e^{-a_r(T-t)}\right) \\ + \sigma_r \int_t^T e^{-a_r(T-s)}\, dW_r^{\mathbb{P}}(s). \end{aligned} \tag{3.4}$$

Similarly, we can write $C_r(t,T)$ and $D_r(t,T)$ as follows:

$$\begin{aligned} D_r(t,T) &:= \frac{1}{a_r}\left(1 - e^{-a_r(T-t)}\right), \\ C_r(t,T) &:= -\frac{\sigma_r^2 D_r^2(t,T)}{4a_r} + \frac{\big(D_r(t,T) - (T-t)\big)\big(a_r(b_r - \rho_{rI}\sigma_I\sigma_r - \sigma_r\lambda_r) - \frac{1}{2}\sigma_r^2\big)}{a_r^2}. \end{aligned}$$

Thus we can compute the distribution of $r_r(T)|\mathcal{F}_t$ with:

$$\begin{aligned}\mathbb{E}_{\mathbb{P}}\left[r_r(T)|\mathcal{F}_t\right] &= r_r(t) + \big(b_r - \rho_{rI}\sigma_I\sigma_r - \sigma_r\lambda_r - a_r r_r(t)\big)D_r(t,T),\\ \mathbb{V}_{\mathbb{P}}\left[r_r(T)|\mathcal{F}_t\right] &= \frac{\sigma_r^2}{2}D_r(2t,2T).\end{aligned} \tag{3.5}$$

3.3.2 Independent Dynamics

Recall from equation (2.28) that the independent $\mathbb{P}$-dynamics for the real short rate are as follows:

$$\begin{aligned}dr_r(t) &= \left[b_r - \tilde{\Sigma}_2\cdot\tilde{\Sigma}_3 - \tilde{\Sigma}_2\tilde{\Lambda} - a_r r_r(t)\right]\,dt + \tilde{\Sigma}_2\,d\tilde{W}^{\mathbb{P}}(t)\\ &= \left[b_r - \tilde{\Sigma}_2\cdot\tilde{\Sigma}_3 - \tilde{\Sigma}_2\tilde{\Lambda} - a_r r_r(t)\right]\,dt + \tilde{\sigma}_{21}\,d\tilde{W}_1^{\mathbb{P}}(t) + \tilde{\sigma}_{22}\,d\tilde{W}_2^{\mathbb{P}}(t) + \tilde{\sigma}_{23}\,d\tilde{W}_3^{\mathbb{P}}(t).\end{aligned}$$

Following the same approach as in section 3.2.2, we can write the solution to this stochastic differential equation as:

$$\begin{aligned}r_r(T) = e^{-a_r(T-t)}r_r(t) &+ \frac{b_r - \tilde{\Sigma}_2\cdot\tilde{\Sigma}_3 - \tilde{\Sigma}_2\tilde{\Lambda}}{a_r}\left(1 - e^{-a_r(T-t)}\right)\\ &+ \tilde{\sigma}_{21}\int_t^T e^{-a_r(T-s)}\,d\tilde{W}_1^{\mathbb{P}}(s) + \tilde{\sigma}_{22}\int_t^T e^{-a_r(T-s)}\,d\tilde{W}_2^{\mathbb{P}}(s)\\ &+ \tilde{\sigma}_{23}\int_t^T e^{-a_r(T-s)}\,d\tilde{W}_3^{\mathbb{P}}(s).\end{aligned}$$

and thus we can write the simulated value for $r_r(T)|\mathcal{F}_t$ as:

$$\begin{aligned}r_r(T) = r_r(t) &+ \big(b_r - \tilde{\Sigma}_2\cdot\tilde{\Sigma}_3 - \tilde{\Sigma}_2\tilde{\Lambda} - a_r r_r(t)\big)D_r(t,T)\\ &+ \tilde{\sigma}_{21}\sqrt{\tfrac{1}{2}D_r(2t,2T)}\tilde{Z}_{1,t} + \tilde{\sigma}_{22}\sqrt{\tfrac{1}{2}D_r(2t,2T)}\tilde{Z}_{2,t}\\ &+ \tilde{\sigma}_{23}\sqrt{\tfrac{1}{2}D_r(2t,2T)}\tilde{Z}_{3,t},\end{aligned} \tag{3.6}$$

where $\tilde{Z}_{1,t} \sim N(0,1)$, $\tilde{Z}_{2,t} \sim N(0,1)$ and $\tilde{Z}_{3,t} \sim N(0,1)$ are the same independent normal variates used to generate $r_n(T)|\mathcal{F}_t$.

3.4 Simulation of the CPI

Simulation of the CPI differs from the simulation of the nominal and the real short rate in that the CPI is assumed to follow a geometric Brownian motion (as opposed to the short rates following Vasiček dynamics) albeit with a time dependent drift. As such, the method of solving the stochastic differential equation for the CPI is slightly more involved. Thus we will not follow the same approach as in the nominal and real short rate in that we will not be providing equations for both the correlated and independent characterisation of the $\mathbb{P}$-dynamics for CPI, and we will

rather only focus on the independent characterisation. This aligns with our overall strategy of using the independent dynamics to simulate each of $r_n(t)$, $r_r(t)$ and $I(t)$, and only requiring the correlated dynamics of $r_n(t)$, $r_r(t)$ in estimation. However, as the derivation itself is quite lengthy, we will only be highlighting the key points in the derivation, and referencing the relevant appendices where necessary.

3.4.1 Independent Dynamics

Recall from equation (2.29) that the independent $\mathbb{P}$-dynamics of the CPI are as follows:

$$\begin{aligned}\frac{dI(t)}{I(t)} &= \left[r_n(t) - r_r(t) - \tilde{\Sigma}_3\tilde{\Lambda}\right]\, dt + \tilde{\Sigma}_3\, d\tilde{W}^{\mathbb{P}}(t) \\ &= \left[r_n(t) - r_r(t) - \tilde{\Sigma}_3\tilde{\Lambda}\right]\, dt + \tilde{\sigma}_{31}\, d\tilde{W}_1^{\mathbb{P}}(t) + \tilde{\sigma}_{32}\, d\tilde{W}_2^{\mathbb{P}}(t) + \tilde{\sigma}_{33}\, d\tilde{W}_3^{\mathbb{P}}(t).\end{aligned}$$

Following the approach provided in Björk (2009), we can arrive at the following solution using Itô's lemma:

$$\begin{aligned}I(T) = I(t)\exp\Bigg[&\int_t^T r_n(s)\, ds - \int_t^T r_r(s)\, ds - \left(\tilde{\Sigma}_3\tilde{\Lambda} + \tfrac{1}{2}\|\tilde{\Sigma}_3\|^2\right)(T-t) \\ &+ \tilde{\sigma}_{31}\left(\tilde{W}_1^{\mathbb{P}}(T) - \tilde{W}_1^{\mathbb{P}}(t)\right) + \tilde{\sigma}_{32}\left(\tilde{W}_2^{\mathbb{P}}(T) - \tilde{W}_2^{\mathbb{P}}(t)\right) + \tilde{\sigma}_{33}\left(\tilde{W}_3^{\mathbb{P}}(T) - \tilde{W}_3^{\mathbb{P}}(t)\right)\Bigg].\end{aligned} \tag{3.7}$$

The proof is contained in Appendix B.1. In order to find the distribution of $I(T)|\mathcal{F}_t$, we first need to find distributions of $\int_t^T r_n(s)\, ds|\mathcal{F}_t$, $-\int_t^T r_r(s)\, ds|\mathcal{F}_t$ and $\tilde{W}_i^{\mathbb{P}}(T) - \tilde{W}_i^{\mathbb{P}}(t)\big|\mathcal{F}_t$ for $i \in \{1,2,3\}$. Beginning with the simplest case first, using the independent increment property of a Wiener process as documented in Björk (2009) we can show that:

$$\tilde{W}_i^{\mathbb{P}}(T) - \tilde{W}_i^{\mathbb{P}}(t)\big|\mathcal{F}_t \sim N\big(0, T-t\big), \qquad \text{for } i \in \{1,2,3\}. \tag{3.8}$$

This allows us to write $\tilde{\sigma}_{3i}\big(\tilde{W}_i^{\mathbb{P}}(T) - \tilde{W}_i^{\mathbb{P}}(t)\big)$ in terms of the independent $\tilde{Z}_{1,t} \sim N(0,1)$, $\tilde{Z}_{2,t} \sim N(0,1)$ and $\tilde{Z}_{3,t} \sim N(0,1)$ as follows:

$$\tilde{\sigma}_{31}\left(\tilde{W}_1^{\mathbb{P}}(T) - \tilde{W}_1^{\mathbb{P}}(t)\right) = \tilde{\sigma}_{31}\sqrt{T-t}\tilde{Z}_{1,t}, \tag{3.9}$$

$$\tilde{\sigma}_{32}\left(\tilde{W}_2^{\mathbb{P}}(T) - \tilde{W}_2^{\mathbb{P}}(t)\right) = \tilde{\sigma}_{32}\sqrt{T-t}\tilde{Z}_{2,t}, \tag{3.10}$$

$$\tilde{\sigma}_{33}\left(\tilde{W}_3^{\mathbb{P}}(T) - \tilde{W}_3^{\mathbb{P}}(t)\right) = \tilde{\sigma}_{33}\sqrt{T-t}\tilde{Z}_{3,t}. \tag{3.11}$$

Now, we turn our attention to the distributions of $\int_t^T r_n(s)\, ds|\mathcal{F}_t$ and $\int_t^T r_r(s)\, ds|\mathcal{F}_t$. In Appendix B.1 we show that we can write:

$$\begin{aligned}\int_t^T r_n(s)\, ds = r_n(t)D_n(t,T) + \frac{b_n - \tilde{\Sigma}_1\tilde{\Lambda}}{a_n}\left[(T-t) - D_n(t,T)\right] \\ + \sum_{i=1}^{3}\left[\tilde{\sigma}_{1i}\int_t^T D_n(s,T)\, d\tilde{W}_i^{\mathbb{P}}(s)\right].\end{aligned} \tag{3.12}$$

And since $D_n(s,T)$ is a deterministic function, we can show by the property of an Itô integral:

$$\int_t^T D_n(s,T)\, d\tilde{W}_i^{\mathbb{P}}(s) \sim N\left(0, \int_t^T D_n(s,T)^2\, ds\right).$$

Evaluating this integral:

$$\begin{aligned}\int_t^T D_n(s,T)^2\, ds &= \int_t^T \frac{1}{a_n^2}\left(1 - e^{-a_n(T-s)}\right)^2 ds \\ &= \frac{1}{a_n^2}\int_t^T 1 - 2e^{-a_n(T-s)} + e^{-2a_n(T-s)}\, ds \\ &= \frac{1}{a_n^2}\left[(T-t) - 2D_n(t,T) + \frac{1}{2}D_n(2t,2T)\right].\end{aligned}$$

Thus, we can simulate a value for $\int_t^T r_n(s)\, ds|\mathcal{F}_t$ using the independent $\tilde{Z}_{1,t}$, $\tilde{Z}_{2,t}$, and $\tilde{Z}_{3,t}$ in the following way:

$$\begin{aligned}\int_t^T r_n(s)\, ds = r_n(t)D_n(t,T) &+ \frac{b_n - \tilde{\Sigma}_1\tilde{\Lambda}}{a_n}\left[(T-t) - D_n(t,T)\right] \\ &+ \frac{\tilde{\sigma}_{11}}{a_n}\sqrt{(T-t) - 2D_n(t,T) + \frac{1}{2}D_n(2t,2T)}\,\tilde{Z}_{1,t} \\ &+ \frac{\tilde{\sigma}_{12}}{a_n}\sqrt{(T-t) - 2D_n(t,T) + \frac{1}{2}D_n(2t,2T)}\,\tilde{Z}_{2,t} \\ &+ \frac{\tilde{\sigma}_{13}}{a_n}\sqrt{(T-t) - 2D_n(t,T) + \frac{1}{2}D_n(2t,2T)}\,\tilde{Z}_{3,t}.\end{aligned} \tag{3.13}$$

Following the exact same approach, we can arrive at the following solution for $\int_t^T r_r(s)\, ds$:

$$\begin{aligned}\int_t^T r_r(s)\, ds = r_r(t)D_r(t,T) &+ \frac{b_r - \tilde{\Sigma}_2\cdot\tilde{\Sigma}_3 - \tilde{\Sigma}_2\tilde{\Lambda}}{a_n}\left[(T-t) - D_r(t,T)\right] \\ &+ \sum_{i=1}^{3}\left[\tilde{\sigma}_{2i}\int_t^T D_r(s,T)\, d\tilde{W}_i^{\mathbb{P}}(s)\right],\end{aligned}$$

which allows us to simulate a value for $\int_t^T r_r(s)\, ds|\mathcal{F}_t$ in terms of the independent $\tilde{Z}_{1,t}$, $\tilde{Z}_{2,t}$ and $\tilde{Z}_{3,t}$ in the following way:

$$\begin{aligned}\int_t^T r_r(s)\, ds = r_r(t)D_r(t,T) &+ \frac{b_r - \tilde{\Sigma}_2\cdot\tilde{\Sigma}_3 - \tilde{\Sigma}_2\tilde{\Lambda}}{a_r}\left[(T-t) - D_r(t,T)\right] \\ &+ \frac{\tilde{\sigma}_{21}}{a_r}\sqrt{(T-t) - 2D_r(t,T) + \frac{1}{2}D_r(2t,2T)}\,\tilde{Z}_{1,t} \\ &+ \frac{\tilde{\sigma}_{22}}{a_r}\sqrt{(T-t) - 2D_r(t,T) + \frac{1}{2}D_r(2t,2T)}\,\tilde{Z}_{2,t} \\ &+ \frac{\tilde{\sigma}_{23}}{a_r}\sqrt{(T-t) - 2D_r(t,T) + \frac{1}{2}D_r(2t,2T)}\,\tilde{Z}_{3,t}.\end{aligned} \tag{3.14}$$

Now, since we have derived the distributions of $\int_t^T r_n(s)\,ds|\mathcal{F}_t$, $\int_t^T r_r(s)\,ds|\mathcal{F}_t$ and $\tilde{W}_i^{\mathbb{P}}(T) - \tilde{W}_i^{\mathbb{P}}(t)\big|\mathcal{F}_t$, we are now ready to derive the distribution of $I(T)|\mathcal{F}_t$. Substituting equations (3.9), (3.10), (3.11), (3.13) and (3.14) into equation (3.7), and making use of the independent normal variates $\tilde{Z}_{1,t}$, $\tilde{Z}_{2,t}$ and $\tilde{Z}_{3,t}$, we are able to write the following large equation to generate a realisation of $I(T)|\mathcal{F}_t$:

$$\begin{aligned} I(T) = I(t)\exp\Bigg[& -\big(\tilde{\Sigma}_3\tilde{\Lambda} + \tfrac{1}{2}\|\tilde{\Sigma}_3\|^2\big)(T-t) \\ & + r_n(t)D_n(t,T) + \frac{b_n - \tilde{\Sigma}_1\tilde{\Lambda}}{a_n}\big[(T-t) - D_n(t,T)\big] \\ & + \frac{1}{a_n}\sqrt{(T-t) - 2D_n(t,T) + \frac{1}{2}D_n(2t,2T)}\sum_{i=1}^{3}\tilde{\sigma}_{1i}\tilde{Z}_{i,t} \\ & - r_r(t)D_r(t,T) - \frac{b_r - \tilde{\Sigma}_2\cdot\tilde{\Sigma}_3 - \tilde{\Sigma}_2\tilde{\Lambda}}{a_r}\big[(T-t) - D_r(t,T)\big] \\ & - \frac{1}{a_r}\sqrt{(T-t) - 2D_r(t,T) + \frac{1}{2}D_r(2t,2T)}\sum_{i=1}^{3}\tilde{\sigma}_{2i}\tilde{Z}_{i,t} \\ & + \sqrt{T-t}\sum_{i=1}^{3}\tilde{\sigma}_{3i}\tilde{Z}_{i,t}\Bigg]. \end{aligned} \tag{3.15}$$

3.5 A Simulated Demonstration of the Model

In this section, we will demonstrate the simulation ability of the model. Firstly, when specifying the model parameters, we will be using parameters similar to those estimated from the US government bond market in Jarrow and Yildirim (2003) so as to mimic the inflation-linked and nominal bond market as closely possible. The input parameters are displayed in table 3.1. As discussed, an important fea-

Tab. 3.1: Model input parameters for the simulated demonstration.

a_n	b_n	σ_n	λ_n	a_r	b_r	σ_r	λ_r	σ_I	λ_I
0.035	0.003575	0.01	0.2	0.045	0.00115	0.005	0.1	0.0125	0.25

ture of the model is the ability to specify the correlations between the processes for $r_n(t)$, $r_r(t)$ and $I(t)$. We again specify these correlations in accordance to the findings in Jarrow and Yildirim (2003) to recover the dynamics of the US government bond market, and display them in table 3.2.

Now, because of how we have specified the dynamics of $r_n(t)$, $r_r(t)$ and $I(t)$ with respect to the independent Brownian motions $d\tilde{W}_1^{\mathbb{P}}(t)$, $d\tilde{W}_2^{\mathbb{P}}(t)$ and $d\tilde{W}_3^{\mathbb{P}}(t)$, we need to specify the model's volatility, correlation and market price of risk pa-

Tab. 3.2: Model input correlations for the simulated demonstration.

ρ_{nr}	ρ_{nI}	ρ_{rI}
0.1	0.2	-0.4

rameters in terms of the matrices $\tilde{\Sigma}$ and $\tilde{\Lambda}$ as defined in section 2.3. By running a least squares optimisation algorithm to find $\tilde{\Sigma}$ such that:

$$\tilde{\Sigma}\tilde{\Sigma}^{\top} = \begin{bmatrix} \sigma_n^2 & \rho_{nr}\sigma_n\sigma_r & \rho_{nI}\sigma_n\sigma_I \\ \rho_{nr}\sigma_n\sigma_r & \sigma_r^2 & \rho_{rI}\sigma_r\sigma_I \\ \rho_{nI}\sigma_n\sigma_I & \rho_{rI}\sigma_r\sigma_I & \sigma_I^2 \end{bmatrix},$$

and $\tilde{\Lambda}$ such that:

$$\tilde{\Sigma}\tilde{\Lambda} = \begin{bmatrix} \sigma_n\lambda_n \\ \sigma_r\lambda_r \\ \sigma_I\lambda_I \end{bmatrix},$$

we arrive at the following matrices:

$$\tilde{\Sigma} = \begin{bmatrix} -0.007121421601678 & 0.006743819963374 & -0.001950960448789 \\ 0.001552619217751 & 0.001039273221270 & -0.004637810338535 \\ 0.002693369890794 & 0.008951897440223 & 0.008298149845062 \end{bmatrix},$$

$$\tilde{\Lambda} = \begin{bmatrix} 0.050619568554014 \\ 0.346177073019886 \\ -0.013289573907189 \end{bmatrix}.$$

We can now use equations (3.3), (3.6) and (3.15) to simulate values for $r_n(t)$, $r_r(t)$ and $I(t)$. For demonstration purposes, we choose $\tau = 8$ such that we work on the time dimension $[0, 8]$. We choose to discretise this dimension evenly into N sub intervals $t_i = \frac{i \times 8}{N}$ for $i \in \{0, 1, ..., N\}$:

$$\left\{ t_0 = 0, t_1 = \tfrac{8}{N}, t_2 = \tfrac{2\times 8}{N}, t_3 = \tfrac{3\times 8}{N}, ..., t_{N-1} = \tfrac{(N-1)\times 8}{N}, t_N = 8 \right\} \tag{3.16}$$

We choose $N = 2000$ such that we will be simulating daily values for the nominal short rate, real short rate, and CPI (corresponding to 250 trading days per year). Note that when simulating, we also choose the following starting values for each simulated component: $r_n(0) = 0.05$, $r_r(0) = 0.02$, and $I(0) = 100$. A plot of one simulated sample path for $r_n(t)$, $r_r(t)$ and $I(t)$ has been produced and is displayed in figure 3.1.

Importantly, note that the correlations ρ_{nr}, ρ_{nI} and ρ_{rI} are preserved in the sim-

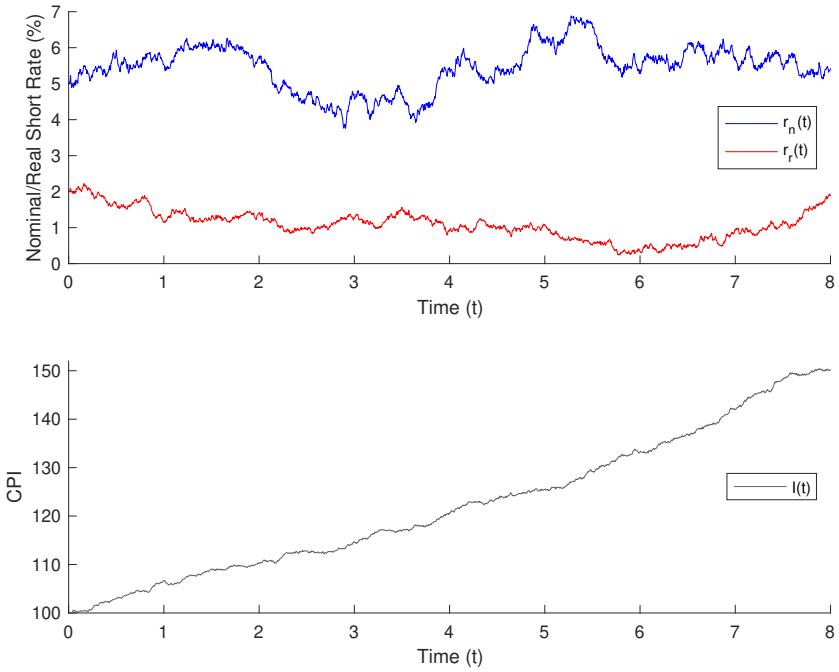

Fig. 3.1: A single simulated sample path for the nominal and real short rates and the CPI.

ulation of model. We can show this by calculating the sample correlations below:

$$\hat{\rho}_{nr} = Corr\left[\Delta r_n(t), \Delta r_r(t)\right],$$
$$\hat{\rho}_{nI} = Corr\left[\Delta r_n(t), \frac{\Delta I(t)}{I(t)}\right],$$
$$\hat{\rho}_{rI} = Corr\left[\Delta r_r(t), \frac{\Delta I(t)}{I(t)}\right].$$

Simulating 1000 distinct sample paths for each process, calculating the above sample correlations, and taking the mean and standard deviation of each estimate allows us to produce table 3.3.

Tab. 3.3: Simulated sample correlations over 1000 sample paths.

Correlation	True Value	Estimated Value	Standard Deviation
ρ_{nr}	0.1	0.10031	0.02220
ρ_{nI}	0.2	0.20084	0.02131
ρ_{rI}	-0.4	-0.39832	0.01809

Lastly, recall from section 3.1 that under the Vasiček model, we have closed form

equations for the nominal and inflation-linked zero-coupon bond prices:

$$P_n(t,T) = e^{C_n(t,T) - D_n(t,T) r_n(t)},$$
$$P_r(t,T) = e^{C_r(t,T) - D_r(t,T) r_r(t)}.$$

For demonstration, we have used the above single simulated sample path for $r_n(t)$ and $r_r(t)$ to produce associated bond prices for chosen constant maturities of 1, 2, 5 and 30 years. A plot of these bond prices has been produced and is displayed in figure 3.2. Note that to ensure legibility, the vertical axes of these plots have not been standardised across the four graphs.

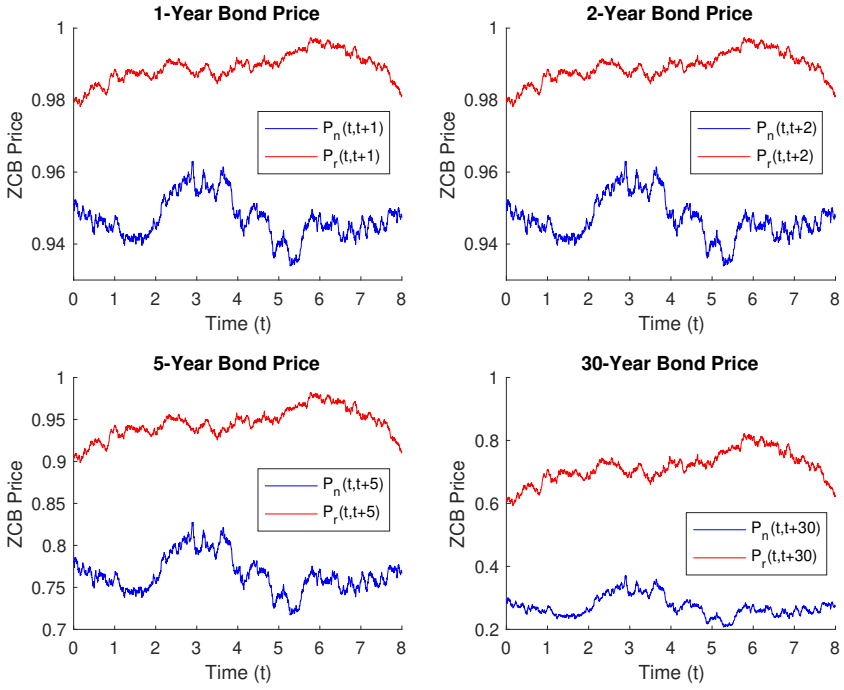

Fig. 3.2: A single simulated sample path for nominal and real zero-coupon bond prices for maturities of 1, 2, 5 and 30 years.

Chapter 4

Estimation and Calibration

As documented by Mercurio (2005) and Belgrade *et al.* (2004), a disadvantage of the models built under the Jarrow and Yildirim (2003) framework is that the parameters are not directly observable in the market. In this chapter, we explain the approach for estimating these unobservable parameters through the use of the Kalman filter, as pioneered by Kalman (1960), and demonstrate its functioning on a simulated data set before applying it to to the South African government bond market. Once the parameters have been estimated, we produce a forecast for break-even inflation under the estimated $\mathbb{P}$-model.

In the final two sections, we implement the general deterministic-shift extension for time-homogeneous short rate models, as described by Brigo and Mercurio (2006), to construct an equivalent model under $\mathbb{Q}$ that is calibrated to observed zero-coupon bond prices at any required time t. We then compare this calibrated $\mathbb{Q}$-model's ability to forecast future inflation to the estimated $\mathbb{P}$-model spoken about above.

4.1 The Kalman Filter

We begin by describing the Kalman filter and its application to interest rate modelling. As documented by Welch and Bishop (1995), the Kalman filter is a set of mathematical equations that provides an efficient computational and recursive solution of the least-squares method. It is well-suited to the area of interest rate modelling since it can be used in estimating past, present and even future states given the information available at the present time, and importantly, it can do so even when the true nature of the underlying modelled system is unobservable (which is typically the case in financial markets).

In this section, we base our explanation of the Kalman filter on the description provided by Bolder (2001), who consolidated the work done by authors Babbs and Nowman (1999), De Jong (2000) and Duan and Simonato (1999) with respect to the

application of the Kalman filter to affine term-structure interest rate models. At a high level, the Kalman filter functions as follows: firstly the interest rate model is required to be cast in its state-space form, which is comprised of two underlying systems of equations: the measurement system and the transition system. In the interest rate modelling case, the measurement system describes the linear relationship between the yield on observable zero-coupon bonds and the underlying short rate. The transition system specifies the unobservable dynamics of the underlying short rate as specified within the interest rate model. The Kalman filter then functions by recursively using the observed zero-coupon yields to infer and update estimates of the true dynamics of the underlying short rate. Lastly, a set of optimal parameters can be produced via maximum likelihood estimation given the observable zero-coupon yields.

4.1.1 The State-Space Formulation

In order to implement the Kalman filter, we are first required to cast our developed short rate model in its state-space form. Recall the nominal and real short rate $\mathbb{P}$-dynamics from equations (2.18) and (2.19):

$$\begin{aligned} dr_n(t) &= [b_n - \sigma_n \lambda_n - a_n r_n(t)]\ dt + \sigma_n\, dW_n^{\mathbb{P}}(t), \\ dr_r(t) &= [b_r - \rho_{rI}\sigma_I \sigma_r - \sigma_r \lambda_r - a_r r_r(t)]\ dt + \sigma_r\, dW_r^{\mathbb{P}}(t). \end{aligned}$$

In this case, we are dealing with two one-factor Vasiček models. Bolder (2001) states that since we are dealing with one-factor models, it is sufficient to use only one zero-coupon yield for each factor to be estimated under the Kalman filter. However, including more than one zero-coupon yield helps increases the cross-sectional information available to the filter and helps to more accurately capture the true unobservable short rate dynamics, especially when estimating their associated market prices of risk. Thus, we will be assuming that M zero-coupon yields are used.

In the same manner as in Chapter 3, we will be discretising the time dimension $[0, \tau]$ into N sub-intervals $t_i = \frac{i \times \tau}{N}$ for $i \in \{0, 1, ..., N\}$ (see equation (3.16)). We will also denote $\Delta t := t_i - t_{i-1}$. In order to infer the zero-coupon yields, we will thus require the following $M \times (N+1)$ matrix of zero-coupon bond prices for $x \in \{n, r\}$:

$$\begin{bmatrix} P_x(t_0, T_1) & P_x(t_1, t_1 + T_1) & \cdots & P_x(t_N, t_N + T_1) \\ P_x(t_0, T_2) & P_x(t_1, t_1 + T_2) & \cdots & P_x(t_N, t_1 + T_2) \\ \vdots & \vdots & \ddots & \vdots \\ P_x(t_0, T_M) & P_x(t_1, t_1 + T_M) & \cdots & P_x(t_N, t_N + T_M) \end{bmatrix},$$

where $T_1, T_2, ..., T_M$ are the M maturities of the observed zero-coupon bonds. Note that these maturities are required to be kept constant through time (for example,

$P_n(t_1, t_1 + T_1)$ corresponds to a T_1-maturity nominal zero-coupon bond observed at time t_1).

Now, given the above matrices of nominal and real zero-coupon bond prices, we can use the following relation to generate the nominal and real continuously compounded zero-coupon bond yields $z_n(t,T)$ and $z_r(t,T)$:

$$z_x(t,T) := -\frac{\ln\big(P_x(t,T)\big)}{T-t}, \quad \text{for } x \in \{n,r\}. \tag{4.1}$$

Importantly, because we have modelled the nominal and real short rate $r_n(t)$ and $r_r(t)$ under the Vasiček model we can write:

$$P_x(t,T) = e^{C_x(t,T) - D_x(t,T) r_x(t)}, \quad \text{for } x \in \{n,r\},$$

and thus we can write $z_x(t,T)$ as follows:

$$z_x(t,T) = \frac{-C_x(t,T) + D_x(t,T) r_x(t)}{T-t}. \tag{4.2}$$

Specification of the Measurement System

Directly from the above definition of $z_x(t,T)$ in terms of the short rates $r_x(t)$ for $x \in \{n,r\}$, we can now write the form of the measurement system. For each $i \in \{1,...,N\}$ and for $x \in \{n,r\}$ we have:

$$\underbrace{\begin{bmatrix} z_x(t_i, t_i+T_1) \\ z_x(t_i, t_i+T_2) \\ \vdots \\ z_x(t_i, t_i+T_M) \end{bmatrix}}_{\mathcal{Z}_x(t_i)} = \underbrace{\begin{bmatrix} -\frac{C_x(t_i,t_i+T_1)}{T_1} \\ -\frac{C_x(t_i,t_i+T_2)}{T_2} \\ \vdots \\ -\frac{C_x(t_i,t_i+T_M)}{T_M} \end{bmatrix}}_{\mathcal{C}_x(t_i)} + \underbrace{\begin{bmatrix} \frac{D_x(t_i,t_i+T_1)}{T_1} \\ \frac{D_x(t_i,t_i+T_2)}{T_2} \\ \vdots \\ \frac{D_x(t_i,t_i+T_M)}{T_M} \end{bmatrix}}_{\mathcal{D}_x(t_i)} r_x(t_i) + \underbrace{\begin{bmatrix} \gamma_{x,1}(t_i) \\ \gamma_{x,1}(t_i) \\ \vdots \\ \gamma_{x,M}(t_i) \end{bmatrix}}_{\Gamma_x(t_i)}.$$

Written concisely in matrix form, we have:

$$\mathcal{Z}_x(t_i) = \mathcal{C}_x(t_i) + \mathcal{D}_x(t_i) r_x(t_i) + \Gamma_x(t_i).$$

In accordance with Bolder (2001), we assume that $\Gamma_x(t_i) \sim N(0, G_x)$ with:

$$G_x = \begin{bmatrix} g^2_{x,1} & 0 & \cdots & 0 \\ 0 & g^2_{x,2} & \cdots & 0 \\ \vdots & \vdots & \ddots & \vdots \\ 0 & 0 & \cdots & g^2_{x,M} \end{bmatrix}.$$

Specification of the Transition System

Recall from Chapter 3 that we provided direct solutions for $r_n(T)|\mathcal{F}_t$ and $r_r(T)|\mathcal{F}_t$ (see equations (3.1) and (3.4)). This allows us to specify the transition system directly, without having to discretise the underlying dynamics through the use of the Euler–Maruyama or Milstein methods (see Brigo and Mercurio (2006)). In the nominal case, for each $i \in \{1, ..., N\}$ we have:

$$r_n(t_i) = \underbrace{(b_n - \sigma_n \lambda_n) D_n(t_{i-1}, t_i)}_{\mathcal{E}_n(t_{i-1})} + \underbrace{e^{-a_n(t_i - t_{i-1})}}_{\mathcal{J}_n(t_{i-1})} r_n(t_{i-1}) + \epsilon_n(t_i),$$

or, in simplified notation:

$$r_n(t_i) = \mathcal{E}_n(t_{i-1}) + \mathcal{J}_n(t_{i-1}) r_n(t_{i-1}) + \epsilon_n(t_i).$$

Directly from equation (3.2), we can write $\epsilon_n(t_i)|\mathcal{F}_{t_{i-1}} \sim N(0, Q_n)$ where:

$$Q_n = \frac{\sigma_n^2}{2} D_n(2t_{i-1}, 2t_i).$$

Similarly, in the real case, for each $i \in \{1, ..., N\}$ we have:

$$r_r(t_i) = \underbrace{(b_n - \rho_{rI}\sigma_I\sigma_r - \sigma_r\lambda_r) D_r(t_{i-1}, t_i)}_{\mathcal{E}_r(t_{i-1})} + \underbrace{e^{-a_r(t_i - t_{i-1})}}_{\mathcal{J}_r(t_{i-1})} r_r(t_{i-1}) + \epsilon_r(t_i),$$

or, in simplified notation:

$$r_r(t_i) = \mathcal{E}_r(t_{i-1}) + \mathcal{J}_r(t_{i-1}) r_r(t_{i-1}) + \epsilon_r(t_i).$$

Again, directly from equation (3.5) we can write $\epsilon_r(t_i)|\mathcal{F}_{t_{i-1}} \sim N(0, Q_r)$ where:

$$Q_r = \frac{\sigma_r^2}{2} D_r(2t_{i-1}, 2t_i).$$

This concludes the state-space formulation of our nominal and real short rate models.

4.1.2 The Kalman Filter Algorithm

In this section, we outline the algorithm provided in Bolder (2001) to implement the Kalman filter to affine term-structure interest rate models, adapted to fit the model specification in this paper.

Step 1: Initialising the Transition System

In order to begin the recursive algorithm, we require initial values for $\mathbb{E}_{\mathbb{P}}\big[r_x(t_0)\big]$ and $\mathbb{V}_{\mathbb{P}}\big[r_x(t_0)\big]$, for $x \in \{n, r\}$. In the same way as Bolder (2001), we use the unconditional expectation and variance of the transition system. In the nominal case we have:

$$\mathbb{E}_{\mathbb{P}}\big[r_n(t_0)\big] = \frac{b_n - \sigma_n \lambda_n}{a_n}, \qquad \mathbb{V}_{\mathbb{P}}\big[r_n(t_0)\big] = \frac{\sigma_n^2}{2a_n},$$

and in the real case we have:

$$\mathbb{E}_{\mathbb{P}}\big[r_r(t_0)\big] = \frac{b_r - \rho_{rI}\sigma_I\sigma_r - \sigma_r\lambda_r}{a_r}, \qquad \mathbb{V}_{\mathbb{P}}\big[r_r(t_0)\big] = \frac{\sigma_r^2}{2a_r}.$$

Step 2: Forecasting the Measurement System

Recall the measurement system for $x \in \{n, r\}$:

$$\mathcal{Z}_x(t_i) = \mathcal{C}_x(t_i) + \mathcal{D}_x(t_i) r_x(t_i) + \Gamma_x(t_i).$$

Taking the expectation and variance given $\mathcal{F}_{t_{i-1}}$, we arrive at the following forecasts:

$$\begin{aligned}
\mathbb{E}_{\mathbb{P}}\left[\mathcal{Z}_x(t_i)\middle|\mathcal{F}_{t_{i-1}}\right] &= \mathcal{C}_x(t_i) + \mathcal{D}_x(t_i)\mathbb{E}_{\mathbb{P}}\left[r_x(t_i)\middle|\mathcal{F}_{t_{i-1}}\right], \\
\mathbb{V}_{\mathbb{P}}\left[\mathcal{Z}_x(t_i)\middle|\mathcal{F}_{t_{i-1}}\right] &= \mathcal{D}_x(t_i)\mathbb{V}_{\mathbb{P}}\left[r_x(t_i)\middle|\mathcal{F}_{t_{i-1}}\right]\mathcal{D}_x(t_i)^{\top} + G_x.
\end{aligned}$$

Step 3: Updating Inference about the Transition System

Firstly, we denote the error in the conditional prediction of the measurement system as $\zeta_x(t_i)$ for $x \in \{n, r\}$ and define it as follows:

$$\zeta_x(t_i) := \mathcal{Z}_x(t_i) - \mathbb{E}_{\mathbb{P}}\left[\mathcal{Z}_x(t_i)\middle|\mathcal{F}_{t_{i-1}}\right],$$

where $\mathcal{Z}_x(t_i)$ are the observed zero-coupon yields. We use this observation to then revise the conditional expectations and variances of the transition system as follows:

$$\mathbb{E}_{\mathbb{P}}\left[r_x(t_i)|\mathcal{F}_{t_i}\right] = \mathbb{E}_{\mathbb{P}}\left[r_x(t_i)\middle|\mathcal{F}_{t_{i-1}}\right] + \mathcal{K}_x(t_i)\zeta_x(t_i), \tag{4.3}$$

$$\mathbb{V}_{\mathbb{P}}\left[r_x(t_i)|\mathcal{F}_{t_i}\right] = \big(1 - \mathcal{K}_x(t_i)\mathcal{D}_x(t_i)\big)\mathbb{V}_{\mathbb{P}}\left[r_x(t_i)\middle|\mathcal{F}_{t_{i-1}}\right], \tag{4.4}$$

where the Kalman gain matrix $\mathcal{K}_x(t_i)$ is defined as follows:

$$\mathcal{K}_x(t_i) = \mathbb{V}_{\mathbb{P}}\left[r_x(t_i)\middle|\mathcal{F}_{t_{i-1}}\right]\mathcal{D}_x(t_i)^{\top}\left[\mathbb{V}_{\mathbb{P}}\left[\mathcal{Z}_x(t_i)\middle|\mathcal{F}_{t_{i-1}}\right]\right]^{-1}.$$

To improve the numerical stability of the algorithm, we use the following expression given in Babbs and Nowman (1999) to calculate the inverse of $\mathbb{V}_{\mathbb{P}}\left[\mathcal{Z}_x(t_i)\middle|\mathcal{F}_{t_{i-1}}\right]$:

$$\left[\mathbb{V}_{\mathbb{P}}\left[\mathcal{Z}_x(t_i)\middle|\mathcal{F}_{t_{i-1}}\right]\right]^{-1} = G_x^{-1} - G_x^{-1}\mathcal{D}_x(t_i)\Big(\mathbb{V}_{\mathbb{P}}\left[r_x(t_i)\middle|\mathcal{F}_{t_{i-1}}\right]^{-1} + \mathcal{D}_x(t_i)^{\top}G_x^{-1}\mathcal{D}_x(t_i)\Big)^{-1}\mathcal{D}_x(t_i)^{\top}G_x^{-1}.$$

Step 4: Forecasting the Transition System

We can now use the updated expectation and variance of the transition system to forecast its value at the next time increment. Recall that the transition system is defined as:

$$r_x(t_{i+1}) = \mathcal{E}_x(t_i) + \mathcal{J}_x(t_i)r_x(t_i) + \epsilon_x(t_{i+1}).$$

Therefore:

$$\mathbb{E}_{\mathbb{P}}\left[r_x(t_{i+1})|\mathcal{F}_{t_i}\right] = \mathcal{E}_x(t_i) + \mathcal{J}_x(t_i)\underbrace{\mathbb{E}_{\mathbb{P}}\left[r_x(t_i)|\mathcal{F}_{t_i}\right]}_{\text{Equation (4.3)}},$$

$$\mathbb{V}_{\mathbb{P}}\left[r_x(t_{i+1})|\mathcal{F}_{t_i}\right] = \mathcal{J}_x(t_i)\underbrace{\mathbb{V}_{\mathbb{P}}\left[r_x(t_i)|\mathcal{F}_{t_i}\right]}_{\text{Equation (4.4)}}\mathcal{J}_x(t_i)^{\top} + Q_x.$$

Step 5: Constructing the Likelihood Function

After initialising the transition system in step 1, we iterate on steps 2 to 4 to generate values for $\zeta_x(t_i)$ and $\mathbb{V}_{\mathbb{P}}\left[\mathcal{Z}_x(t_i)\middle|\mathcal{F}_{t_{i-1}}\right]$ for $i \in \{1, ..., N\}$, for $x \in \{n, r\}$. As in Bolder (2001), under the assumption that the measurement system prediction errors $\zeta_x(t_i)$ follow a multi-variate normal distribution we can construct the following log-likelihood function dependent on the input parameters $\theta_x := \{a_x, b_x, \sigma_x, \lambda_x\}$ for $x \in \{n, r\}$:

$$\begin{aligned}\ell\big(\mathcal{Z}_x(t_1), ..., \mathcal{Z}_x(t_N); \theta_x\big) &= \sum_{i=1}^{N} \ln\Big((2\pi)^{-\frac{M}{2}}\left|\mathbb{V}_{\mathbb{P}}\left[\mathcal{Z}_x(t_i)\middle|\mathcal{F}_{t_{i-1}}\right]\right|^{-\frac{1}{2}} \\ &\qquad \times e^{-\frac{1}{2}\zeta_x(t_i)^{\top}\mathbb{V}_{\mathbb{P}}\left[\mathcal{Z}_x(t_i)\middle|\mathcal{F}_{t_{i-1}}\right]^{-1}\zeta_x(t_i)}\Big) \\ &= -\frac{MN\ln(2\pi)}{2} - \frac{1}{2}\sum_{i=1}^{N}\ln\left|\mathbb{V}_{\mathbb{P}}\left[\mathcal{Z}_x(t_i)\middle|\mathcal{F}_{t_{i-1}}\right]\right| \\ &\qquad + \zeta_x(t_i)^{\top}\mathbb{V}_{\mathbb{P}}\left[\mathcal{Z}_x(t_i)\middle|\mathcal{F}_{t_{i-1}}\right]^{-1}\zeta_x(t_i).\end{aligned}$$

Then, to find the parameters θ_x that best fit the observed zero-coupon yields, we make use a non-linear optimisation algorithm to find the optimal parameters $\hat{\theta}_x$

that maximise the above log-likelihood for $x \in \{n, r\}$. Note that to improve numerical stability, we employ the following expression outlined in Babbs and Nowman (1999) to evaluate $\ln\left|\mathbb{V}_{\mathbb{P}}\left[\mathcal{Z}_x(t_i)\middle|\mathcal{F}_{t_{i-1}}\right]\right|$:

$$\begin{aligned}\ln\left|\mathbb{V}_{\mathbb{P}}\left[\mathcal{Z}_x(t_i)\middle|\mathcal{F}_{t_{i-1}}\right]\right| &= \ln\Big(|G_x|\cdot\left|\mathbb{V}_{\mathbb{P}}\left[r_x(t_i)\middle|\mathcal{F}_{t_{i-1}}\right]\right|\cdot \\ &\qquad \left|\mathbb{V}_{\mathbb{P}}\left[r_x(t_i)\middle|\mathcal{F}_{t_{i-1}}\right]^{-1}+\mathcal{D}_x(t_i)^{\top}G_x^{-1}\mathcal{D}_x(t_i)\right|\Big) \\ &= \ln|G_x|+\ln\left|\mathbb{V}_{\mathbb{P}}\left[r_x(t_i)\middle|\mathcal{F}_{t_{i-1}}\right]\right| \\ &\qquad +\ln\left|\mathbb{V}_{\mathbb{P}}\left[r_x(t_i)\middle|\mathcal{F}_{t_{i-1}}\right]^{-1}+\mathcal{D}_x(t_i)^{\top}G_x^{-1}\mathcal{D}_x(t_i)\right|.\end{aligned}$$

By using the fact that G_x is a diagonal matrix, we can further write:

$$\ln|G_x| = \ln\left(\prod_{j=1}^{M} g_{x,j}^2\right) = 2\sum_{j=1}^{M}\ln\left(g_{x,j}\right).$$

For large values of M, the expressions given by Babbs and Nowman (1999) for $\left[\mathbb{V}_{\mathbb{P}}\left[\mathcal{Z}_x(t_i)\middle|\mathcal{F}_{t_{i-1}}\right]\right]^{-1}$ and $\ln\left|\left(\mathbb{V}_{\mathbb{P}}\left[\mathcal{Z}_x(t_i)\middle|\mathcal{F}_{t_{i-1}}\right]\right)\right|$ ensure that evaluating the log-likelihood function does not result in infinite values.

4.2 Estimating on a Simulated Dataset

In this section, we demonstrate the estimation ability of the Kalman filter on the data simulated in Chapter 3. We outline the process followed to construct the dataset required by the algorithm, and highlight the difference in the estimation approach between the parameters that are filterable and those that are not.

4.2.1 Description of the Dataset

As a reminder, we simulated 1000 sample paths of the nominal short rate $r_n(t)$, the real short rate $r_r(t)$ and the CPI $I(t)$ over a time horizon $[0, 8]$. We discretised the time horizon by specifying $N = 2000$ such that each year was split into 250 intervals (corresponding to 250 trading days per year). We can then use equation (4.2) to construct a yield curve at each t_i, with the choice of maturities as follows:

$$\begin{aligned}\Big\{&T_1=\tfrac{1}{365}, && T_2=\tfrac{30}{365}, && T_3=\tfrac{90}{365}, && T_4=\tfrac{120}{365}, && T_5=\tfrac{150}{365}, && T_6=\tfrac{180}{365},\\ &T_7=\tfrac{210}{365}, && T_8=\tfrac{240}{365}, && T_9=\tfrac{270}{365}, && T_{10}=\tfrac{300}{365}, && T_{11}=\tfrac{330}{365}, && T_{12}=1,\\ &T_{13}=\tfrac{455}{365}, && T_{14}=\tfrac{545}{365}, && T_{15}=\tfrac{635}{365}, && T_{16}=2, && T_{17}=3, && T_{18}=4,\\ &\cdots, && T_{28}=14, && T_{29}=15, && T_{30}=20, && T_{31}=25, && T_{32}=30\Big\}.\end{aligned} \tag{4.5}$$

This choice of maturities has been made so as to be consistent with the South African yield curve data available (to be discussed in section 4.3). Thus we have

$M = 32$ maturities of observed zero-coupon continuously compounded bond yields, and can construct our $M \times (N+1)$ matrix of yields as follows for $x \in \{n, r\}$:

$$\begin{bmatrix} z_x(t_0, t_0+T_1) & z_x(t_1, t_1+T_1) & \cdots & z_x(t_{2000}, t_{2000}+T_1) \\ z_x(t_0, t_0+T_2) & z_x(t_1, t_1+T_2) & \cdots & z_x(t_{2000}, t_{2000}+T_2) \\ \vdots & \vdots & \ddots & \vdots \\ z_x(t_0, t_0+T_{32}) & z_x(t_1, t_1+T_{32}) & \cdots & z_x(t_{2000}, t_{2000}+T_{32}) \end{bmatrix}.$$

We will also have a $1 \times (N+1)$ matrix of CPI values:

$$\begin{bmatrix} I(t_0) & I(t_1) & \cdots & I(t_{2000}) \end{bmatrix}.$$

4.2.2 Estimation of Non-Filterable Parameters

In running the Kalman filter, we will be able to estimate the parameters $\theta_n = \{a_n, b_n, \sigma_n, \lambda_n\}$ and $\theta_r = \{a_r, b_r, \sigma_r, \lambda_r\}$. This does not however include the estimation of the correlation parameters $\{\rho_{nr}, \rho_{nI}, \rho_{rI}\}$ or the CPI process parameters $\{\sigma_I, \lambda_I\}$, which are required to fully specify the model. We term these parameters "non-filterable", referring to the fact that under our implementation of the Kalman filter we are unable to recover these parameters. This is, however, not an insurmountable issue as we can simply use sample estimates to recover the correlation parameters and σ_I, which is exactly the method employed in Jarrow and Yildirim (2003). The reasoning for this chosen approach is that the CPI process $I(t)$ itself can be directly observed (as opposed to $r_n(t)$ and $r_r(t)$ which cannot), and as such there is not as great of a need to incorporate $I(t)$ into our implementation of the Kalman filter to estimate its associated parameters.[1]

It must be noted however, that under our model specification it will not be possible to recover λ_I using sample estimates, which means that under $\mathbb{P}$, we will not be able to simulate values for the CPI process $I(t)$. As will still be discussed however, we are still able to generate estimates of break-even inflation under $\mathbb{P}$ without having to simulate $I(t)$.

We have already defined the sample estimates of the correlations in Chapter 3, however there they are defined in terms of $\Delta r_n(t)$ and $\Delta r_r(t)$ so let us adjust their

[1] It must be emphasised that it would be possible to incorporate $I(t)$ in the developed Kalman filter and in this way estimate these "non-filterable" parameters, however we have chosen to avoid this approach as it would complicate the Kalman filter unnecessarily, as the method of sample estimates is sufficient for our purposes.

definition by noting that:

$$z_x(t+\Delta t, T+\Delta t) - z_x(t,T) = \frac{D_x(t,T)\big(r_x(t+\Delta t) - r_x(t)\big)}{T-t},$$
$$\therefore \Delta r_x(t) = \frac{(T-t)\Delta z_x(t,T)}{D_x(t,T)}.$$

And since $(T-t)$ and $D_x(t,T)$ are constants, by covariance laws we can show:

$$\hat{\rho}_{nr} = \text{Corr}\big[\Delta r_n(t), \Delta r_r(t)\big] = \text{Corr}\big[\Delta z_n(t,T), \Delta z_r(t,T)\big], \tag{4.6}$$
$$\hat{\rho}_{nI} = \text{Corr}\left[\Delta r_n(t), \frac{\Delta I(t)}{I(t)}\right] = \text{Corr}\big[\Delta z_n(t,T), \frac{\Delta I(t)}{I(t)}\big], \tag{4.7}$$
$$\hat{\rho}_{rI} = \text{Corr}\left[\Delta r_r(t), \frac{\Delta I(t)}{I(t)}\right] = \text{Corr}\big[\Delta z_r(t,T), \frac{\Delta I(t)}{I(t)}\big]. \tag{4.8}$$

The proofs of these equations are contained in Appendix C.1. Note that in the above equations, the value of T does not change the correlation value, and thus we can compute $\hat{\rho}_{nr}$, $\hat{\rho}_{nI}$ and $\hat{\rho}_{rI}$ for any T_j, $j \in \{1,2,3,...,M\}$. Thus we can redefine our sample correlations in terms of the simulated yields:

$$\hat{\rho}_{nr} = \text{Corr}\big[\Delta z_n(t, t+T_j), \Delta z_r(t, t+T_j)\big], \tag{4.9}$$
$$\hat{\rho}_{nI} = \text{Corr}\left[\Delta z_n(t, t+T_j), \frac{\Delta I(t)}{I(t)}\right], \tag{4.10}$$
$$\hat{\rho}_{rI} = \text{Corr}\left[\Delta z_r(t, t+T_j), \frac{\Delta I(t)}{I(t)}\right], \tag{4.11}$$

for any $j \in \{1,2,3,...,M\}$. We define the sample estimate of σ_I for in accordance with Jarrow and Yildirim (2003) as follows:

$$\hat{\sigma}_I = \sqrt{\frac{1}{\Delta t}\,\text{Var}\left[\frac{\Delta I(t)}{I(t)}\right]}. \tag{4.12}$$

Computing these estimates over 100 sample paths, we obtain table 4.1. It can be seen that the method of sample estimates is sufficient in recovering each of the parameters $\{\rho_{nr}, \rho_{nI}, \rho_{rI}, \sigma_I\}$, as evidenced by the low standard deviations for each estimate.

4.2.3 Estimation Using the Kalman Filter

Now that we have estimated the non-filterable parameters $\{\rho_{nr}, \rho_{nI}, \rho_{rI}, \sigma_I\}$, we can estimate $\theta_n = \{a_n, b_n, \sigma_n, \lambda_n\}$ and $\theta_r = \{a_r, b_r, \sigma_r, \lambda_r\}$ through the Kalman filter. Note that because we are dealing with simulated data, we choose $g_{x,j} = 0.001$ for

Tab. 4.1: Non-filterable parameter estimates produced using 100 sample paths of the simulated dataset.

Parameter	True Value	Estimated Value	Standard Deviation
$\hat{\rho}_{nr}$	0.1	0.100170	0.023189
$\hat{\rho}_{nI}$	0.2	0.202968	0.021782
$\hat{\rho}_{rI}$	-0.4	-0.400138	0.018298
$\hat{\sigma}_I$	0.0125	0.012535	0.000191

all $j \in \{1, 2, ..., M\}$, i.e.:

$$G_x = \begin{bmatrix} 0.001^2 & 0 & \cdots & 0 \\ 0 & 0.001^2 & \cdots & 0 \\ \vdots & \vdots & \ddots & \vdots \\ 0 & 0 & \cdots & 0.001^2 \end{bmatrix}, \qquad \text{for } x \in \{n, r\}.$$

Running the Kalman filter on the same 100 sample paths as was previously simulated, we obtain the following estimates presented in table 4.2.

Tab. 4.2: Parameter estimates produced by the Kalman filter using 100 sample paths of the simulated dataset.

Parameter	True Value	Estimated Value	S.Dev
$\hat{a}_n$	0.035	0.034989	0.000180
$\hat{b}_n$	0.003575	0.003735	0.000110
$\hat{\sigma}_n$	0.01	0.009996	0.000042
$\hat{\lambda}_n$	0.2	0.216193	0.010676
$\hat{a}_r$	0.045	0.044990	0.000484
$\hat{b}_r$	0.00115	0.001169	0.000055
$\hat{\sigma}_r$	0.005	0.004983	0.000071
$\hat{\lambda}_r$	0.1	0.104266	0.009989

It can be seen that the Kalman filter performs well when estimating the parameters $\{a_n, b_n, \sigma_n\}$ and $\{a_r, b_r, \sigma_r\}$, estimating each quite closely and with a low standard deviation. However, the Kalman filter appears to experience some difficulty in correctly estimating the market price of risk parameters λ_n and λ_r, as both are the estimates with the highest standard deviations (both in absolute and relative terms). This is not completely unexpected however as Bolder (2001) also found that the market price of risk parameters were the ones most difficult to estimate through the Kalman filter. This is further and more generally documented in Duffee and

Stanton (2012) where it is shown that for a number of different interest rate models, the market price of risk parameters are the ones most difficult to estimate.

We are also able to plot the estimates of the yields produced by the Kalman filter, $\mathbb{E}_{\mathbb{P}}\left[\mathcal{Z}_x(t_i)\middle|\mathcal{F}_{t_{i-1}}\right]$, which are then used in step 3 of the algorithm to update the inference about the transition system. For the sake of exposition, we have plotted the nominal and real 1-year, 2-year, 5-year and 30-year continuously compounded yields inputted to the Kalman filter, and the outputted estimates $\mathbb{E}_{\mathbb{P}}\left[\mathcal{Z}_x(t_i)\middle|\mathcal{F}_{t_{i-1}}\right]$ in figure 4.1. What we are really interested in, however, is the Kalman filter's abil-

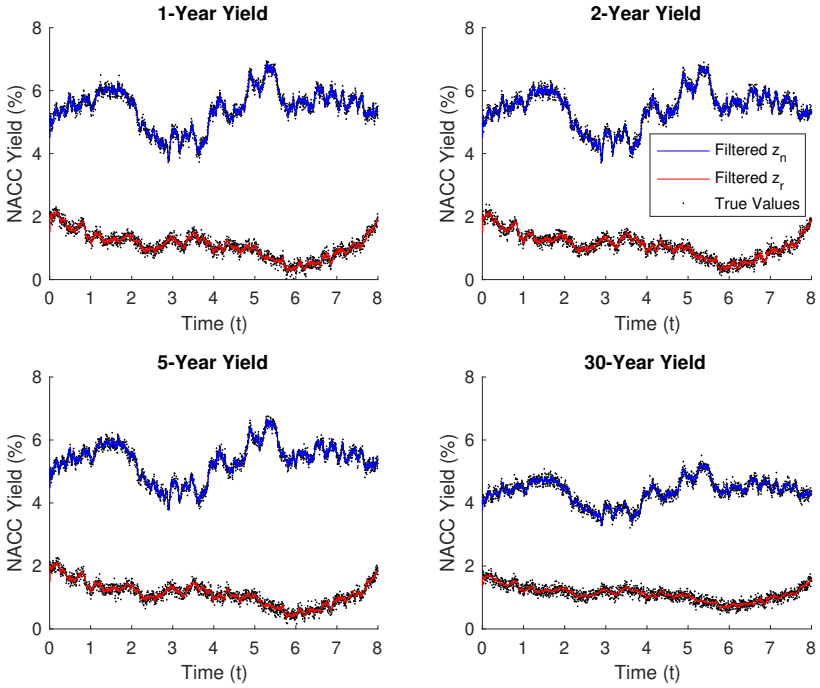

Fig. 4.1: Simulated nominal and real zero-coupon bond yields, estimated via Kalman filter.

ity to reproduce the true underlying short rate dynamics. In figure 4.2 we plot the updated estimates of the transition system $\mathbb{E}_{\mathbb{P}}\left[r_x(t_i)|\mathcal{F}_{t_i}\right]$ against the true simulated dynamics for $r_n(t)$ and $r_r(t)$. As can be seen, the Kalman filter recovers these dynamics to a high degree of accuracy.

4.3 Estimating Using South African Bond Data

In this section, we apply the estimation process outlined in section 4.2 to South African government bond data. In the same way, we first describe the dataset used

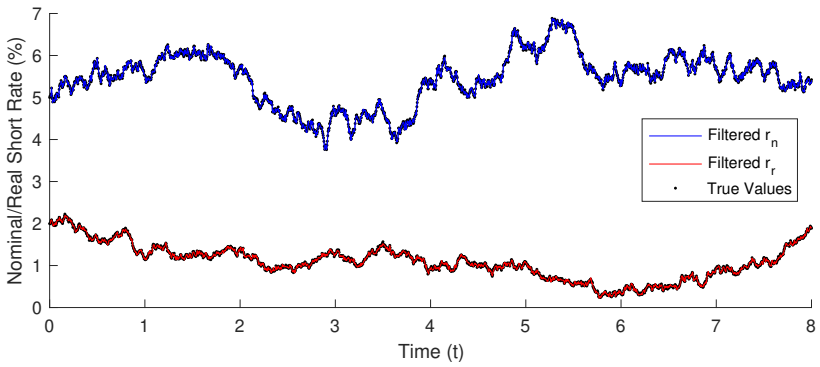

Fig. 4.2: Simulated nominal and real short rates, estimated via Kalman filter.

to conduct estimation, and discuss the treatment of the parameters that are filterable and those that are not.

4.3.1 Description of the Dataset

We have access to both nominal and real continuously compounded yield curve data from 30-Sep-2013 to 30-Sep-2021. This corresponds to $N = 1989$ time indices over the 8 year period (which equates to approximately 250 trading days per year). The yield curve maturities are exactly the same as discussed in section 4.2 (see equation (4.5)). Importantly, because the times indices t_i are for set dates during the year, Δt is not constant. This is however easily dealt with in both the estimation of the non-filterable parameters and the parameters estimated via Kalman filter.

We also have access to monthly CPI headline figures from Jan-1980 to Dec-2021, obtained from StatsSA.[2] To ensure consistency with the nominal and real data available, we will only be using the CPI figures from May-2013 to May-2021 (to account for the 4-month time lag). This results in 97 data points for the CPI.

4.3.2 Estimation of Non-Filterable Parameters

Following the same process as in section 4.2, we first begin by estimating the non-filterable parameters ρ_{nr}, ρ_{nI}, ρ_{rI} and σ_I. We will thus be using the same sample estimate formulae as in equations 4.9, 4.10, 4.11 and 4.12. Since we have maturities T_j for $j \in \{1, 2, ..., M\}$, we will produce M estimates for $\hat{\rho}_{nr}$, $\hat{\rho}_{nI}$ and $\hat{\rho}_{rI}$, which we will then take the mean and standard deviation of. This was not required when estimating on the simulated dataset as regardless of the choice of T_j, the correlation

[2] These figures are publicly available at the following URL: http://www.statssa.gov.za/?page_id=1854&PPN=P0141&SCH=72746.

was always the same (this is exactly as expected since the only source of randomness in the simulated yields $z_x(t, t+T_j)$ is due to $r_x(t)$, which doesn't change as T_j changes). Taking the mean will allow us to consider the correlations over the entire yield curve, instead of making an arbitrary choice of T_j which may result in correlation estimates which are not representative of the entire dataset. We however cannot do the same for $\hat{\sigma}_I$ since we only have the one realisation of $I(t)$.

Importantly, because we are dealing with monthly CPI data, we will only consider the monthly changes in nominal and real yields (i.e., we choose $\Delta t = \frac{1}{12}$) when calculating $\hat{\rho}_{nI}$ and $\hat{\rho}_{rI}$. As outlined in Jarrow and Yildirim (2003), we avoid interpolating between the monthly CPI figures to produce daily figures as this process is deterministic and will result in a misspecification of the estimate of CPI volatility $\hat{\sigma}_I$ and of the correlations $\hat{\rho}_{nI}$ and $\hat{\rho}_{rI}$. For $\hat{\rho}_{nr}$ we will be using the daily data to produce the most accurate estimate as possible. A collection of the estimates are contained in table 4.3.

Tab. 4.3: Non-filterable parameter estimates produced using South African bond data.

Parameter	Estimated Value	Standard Deviation
$\hat{\rho}_{nr}$	0.080110	0.081550
$\hat{\rho}_{nI}$	0.011571	0.124625
$\hat{\rho}_{rI}$	0.309798	0.176883
$\hat{\sigma}_I$	0.013539	-

Notice that the estimate of ρ_{nr} has the lowest standard deviation, as we have 1989 realisations of $\Delta z_x(t, t+T_j)$ for $x \in \{n, r\}$ over the period 30-Sep-2013 to 30-Sep-2013, as opposed to $\hat{\rho}_{nr}$ and $\hat{\rho}_{nr}$ being calculated on only 97 realisations of $\Delta z_x(t, t+T_j)$ and $\frac{\Delta I(t)}{I(t)}$ over the same period. The estimates of $\hat{\rho}_{nr}$, $\hat{\rho}_{nI}$ and $\hat{\sigma}_I$ are all similar to those found by Jarrow and Yildirim (2003) in the US government bond market. The magnitude of $\hat{\rho}_{rI}$ is also similar, however in the South African government bond market there is a positive correlation between real short rates and inflation, as opposed to the negative correlation observed in the US market.

4.3.3 Estimation Using the Kalman Filter

In the same way as in section 4.2, now that we have estimated the non-filterable parameters $\{\rho_{nr}, \rho_{nI}, \rho_{rI}, \sigma_I\}$, we can begin estimation of $\theta_n = \{a_n, b_n, \sigma_n, \lambda_n\}$ and $\theta_r = \{a_r, b_r, \sigma_r, \lambda_r\}$ through the Kalman filter. One point of difference however, is that since we are not simulating data anymore, we do not assume a fixed value for $g_{x,j}$ for all $j \in \{1, 2, ..., M\}$, and we rather allow the Kalman filter algorithm to

estimate its value. To limit the number of parameters the algorithm must estimate, we do however specify that $g_{x,j} = g_x$ for all $j \in \{1, 2, ..., M\}$, i.e.,

$$G_x = \begin{bmatrix} g_x^2 & 0 & \cdots & 0 \\ 0 & g_x^2 & \cdots & 0 \\ \vdots & \vdots & \ddots & \vdots \\ 0 & 0 & \cdots & g_x^2 \end{bmatrix}.$$

Thus, in the nominal case we will be producing estimates of $\hat{\theta}_n = \{\hat{a}_n, \hat{b}_n, \hat{\sigma}_n, \hat{\lambda}_n\}$ and $\hat{g}_n$, and in the real case we will be producing estimates of $\hat{\theta}_r = \{\hat{a}_r, \hat{b}_r, \hat{\sigma}_r, \hat{\lambda}_r\}$ and $\hat{g}_r$. To reduce the effect of the non-linear optimisation algorithm used getting stuck in local minima, we randomise the initial estimates supplied to the optimiser. We conduct 100 such trials, and calculate the estimates in each. These estimates are contained in table 4.4.

Tab. 4.4: Parameter estimates produced by the Kalman filter using South African bond data.

Parameter	Estimated Value	S.Dev
$\hat{a}_n$	0.231475	0.000002
$\hat{b}_n$	0.026806	0.000909
$\hat{\sigma}_n$	0.006978	0.000001
$\hat{\lambda}_n$	0.119792	0.130273
$\hat{g}_n$	0.008606	0.000001
$\hat{a}_r$	0.000124	0.000139
$\hat{b}_r$	0.003661	0.001625
$\hat{\sigma}_r$	0.012246	0.001657
$\hat{\lambda}_r$	0.109474	0.141665
$\hat{g}_n$	0.005147	0.000087

Notice how, similar to estimating on the simulated dataset, the Kalman filter expresses significantly more difficulty in estimating the parameters λ_n and λ_r in comparison to the the parameters $\{a_n, b_n, \sigma_n\}$ and $\{a_r, b_r, \sigma_r\}$ which almost always converge to the same value regardless of the initial conditions supplied (as evidenced by their low standard deviations).

In figure 4.3, we plot the 1-year, 2-year, 5-year and 30-year nominal and real continuously compounded yield estimates $\mathbb{E}_{\mathbb{P}}\left[\mathcal{Z}_x(t_i)\middle|\mathcal{F}_{t_{i-1}}\right]$ predicted by the Kalman filter. Note that we do not plot the estimates $\mathbb{E}_{\mathbb{P}}\left[r_x(t_i)|\mathcal{F}_{t_i}\right]$ for the short rate since we do not have the true underlying instantaneous short rates to them compare to. Looking at the produced plots, we can see that there is a mismatch between

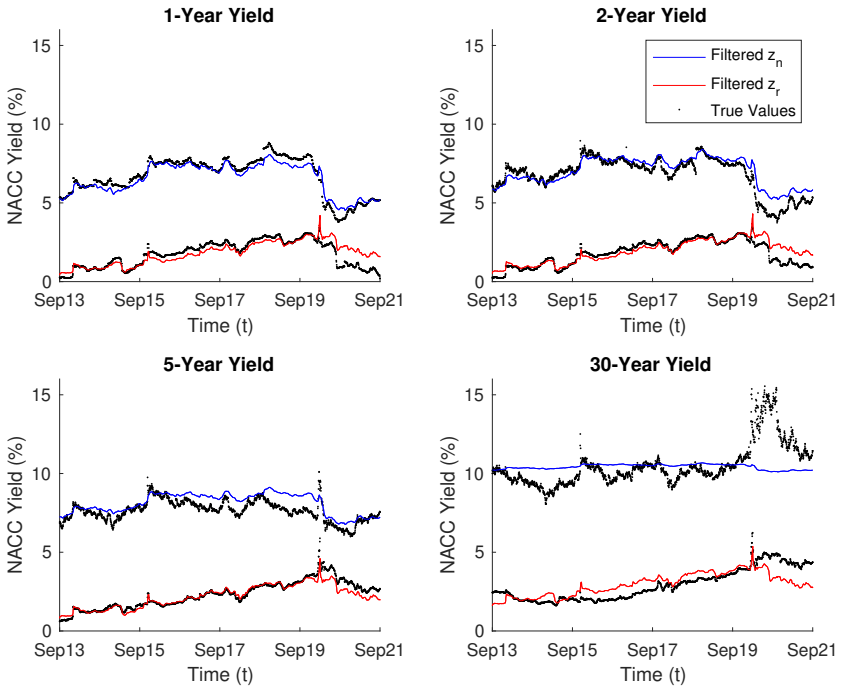

Fig. 4.3: Nominal and real South African zero-coupon bond yields, estimated via Kalman filter.

the estimated and true continuously compounded zero-coupon yields which gets greater as time-to-maturity increases. Particularly, we can see how the model is able to adequately recover the yields for maturities of five years or less (i.e., the short-to-medium-end of the yield curve), but it is then unable to do more than capture the average yield for the long-end of the curve (especially in the nominal case). This can be attributed to the fact that a one-factor Vasiček model is not sufficient to capture the dynamics of the entire yield curve, and as such, we propose that for future research it would be worthwhile to consider a multi-factor Vasiček model for the nominal and real short rate to better aid in yield curve fitting. As for the rest of this dissertation, we will be focusing on the short-to-medium-end of the yield curve (i.e., maturities five years and less) as this is the area where our constructed model's performance is greatest.

4.4 Forecasting Inflation Under the Real-World Measure

In this section, we consider using the estimated model under the real-world measure $\mathbb{P}$ to produce a forecast for future break-even inflation.

4.4.1 Defining Break-Even Inflation

We begin by defining break-even inflation within our constructed model. As we already mentioned in Chapter 2, the Fisher equation is commonly stated as "expected inflation $\approx$ nominal interest rates $-$ real interest rates". Defining i_n as the nominal annual effective interest rate , i_r as the real annual effective interest rate, and π as the annual inflation, we can write the non-approximated version of the Fisher equation as:

$$(1 + i_n) = (1 + \pi)(1 + i_r).$$

By manipulating this equation, we can instead write annual inflation π in terms of zero-coupon bond prices $P_n(t, T)$ and $P_r(t, T)$:

$$\pi = \left(\frac{P_r(t, T)}{P_n(t, T)} \right)^{\frac{1}{T-t}} - 1.$$

Under the estimated model, we are able to simulate T_j-maturity nominal and real bond prices for $j \in \{1, 2, 3, ..., M\}$, and thus we are able to calculate estimates of break-even inflation for each of the M maturities. Thus, let us adjust our notation to emphasise that we are inferring break-even inflation for each T_j:

$$\pi(t; T_j) := \left(\frac{P_r(t, t + T_j)}{P_n(t, t + T_j)} \right)^{\frac{1}{T_j}} - 1. \tag{4.13}$$

To be clear, $\pi(t; T_j)$ can be interpreted as the annual break-even inflation at time t, inferred from T_j-maturity nominal and real zero-coupon bonds.

4.4.2 Forecasting Break-Even Inflation

Using the estimated parameters in table 4.1 and 4.2, and working on the same time horizon of $[0, 8]$ (which we discretise in the same way as usual, see equation (3.16)) where time $t = 0$ corresponds to 30-Sep-2021, we simulate 1000 sample paths of $r_n(t)$ and $r_r(t)$, using the observed overnight yields on 30-Sep-2021 as proxies for $r_n(0)$ and $r_r(0)$. We then use the usual bond maturities defined in equation (4.5) to generate 1000 realisations of the yield curve over the time period $[0, 8]$, which we can then use together with equation (4.13) to produce 1000 realisations of $\pi(t; T_j)$ for each T_j over the same period. We then take the mean and standard deviation of $\pi(t; T_j)$ over all sample paths to generate a forward-looking estimate and 95% confidence interval for break-even inflation over the time period $[0, 8]$. We display our estimates of $\pi(t; 1)$, $\pi(t; 2)$, $\pi(t; 3)$ and $\pi(t; 5)$ in figure 4.4 (which we will discuss when we compare to the estimates generated under $\mathbb{Q}$ in section 4.6.1).

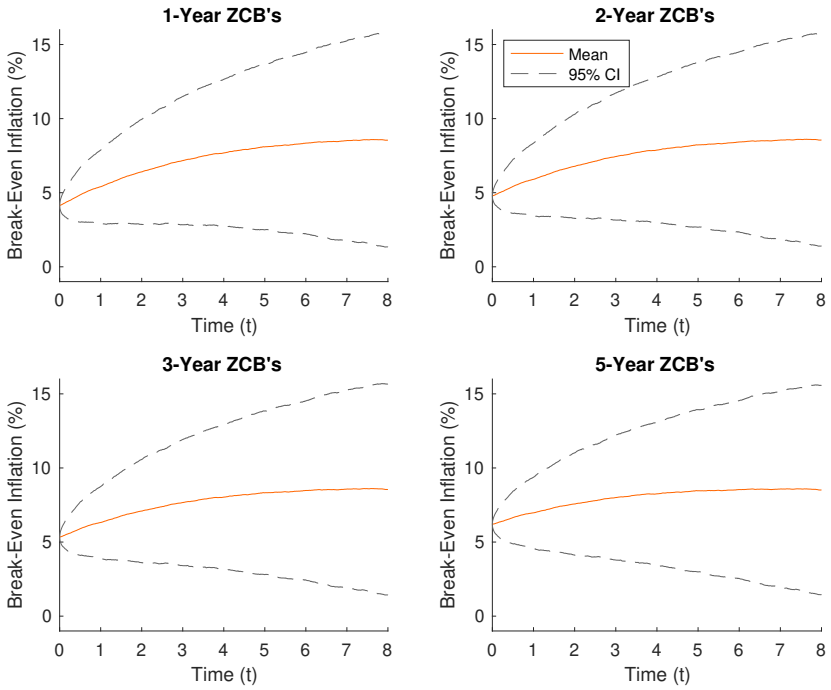

Fig. 4.4: Break-even inflation forecasts inferred from 1-year, 2-year, 3-year and 5-year simulated zero-coupon bonds under the estimated $\mathbb{P}$-model.

4.5 Calibration Using The General Deterministic-Shift Extension

In this section we cover the general deterministic-shift extension for one-factor short rate models, which allows us to extend our time-homogeneous Vasiček models for the nominal and the real short rate such that they are able to exactly reproduce the observed term structure of interest rates on any given day. Using this extension, we will be working under the risk-neutral measure $\mathbb{Q}$ which means that the calibrated model can be used to price financial derivatives (something which would not be possible under the estimated $\mathbb{P}$-model developed previously). We also consider the generation of inflation forecasts under the risk-neutral measure $\mathbb{Q}$ inferred from calibrated bond prices. The derivations contained in this section are built on the procedure outlined in Brigo and Mercurio (2006).

4.5.1 The General Deterministic-Shift Extension

We begin with our time-homogeneous short rate processes under $\mathbb{P}$:

$$dr_n^{\mathbb{P}}(t) = \Big[b_n - \sigma_n\lambda_n - a_n r_n^{\mathbb{P}}(t)\Big]\ dt + \sigma_n\, dW_n^{\mathbb{P}}(t),$$
$$dr_r^{\mathbb{P}}(t) = \Big[b_r - \rho_{rI}\sigma_I\sigma_r - \sigma_r\lambda_r - a_r r_r^{\mathbb{P}}(t)\Big]\ dt + \sigma_r\, dW_r^{\mathbb{P}}(t).$$

For notation's sake, we have added the superscript $^{\mathbb{P}}$ to both short rate processes to signify that these are the dynamics under the real-world measure $\mathbb{P}$. Using the Girsanov transformation as defined in equation (2.4), we can define the equivalent dynamics under the risk-neutral measure $\mathbb{Q}$:

$$dr_n^{\mathbb{Q}}(t) = \Big[b_n - a_n r_n^{\mathbb{Q}}(t)\Big]\ dt + \sigma_n\, dW_n^{\mathbb{Q}}(t),$$
$$dr_r^{\mathbb{Q}}(t) = \Big[b_r - \rho_{rI}\sigma_I\sigma_r - a_r r_r^{\mathbb{Q}}(t)\Big]\ dt + \sigma_r\, dW_r^{\mathbb{Q}}(t).$$

Again, we have used the superscript $^{\mathbb{Q}}$ to differentiate between the short rate processes under the two equivalent measures. We now define the calibrated nominal and real short rate processes under $\mathbb{Q}$ as:

$$r_n^{Cal,\mathbb{Q}}(t) := r_n^{\mathbb{Q}}(t) + \varphi_n(t), \quad t \geq 0, \tag{4.14}$$
$$r_r^{Cal,\mathbb{Q}}(t) := r_r^{\mathbb{Q}}(t) + \varphi_r(t), \quad t \geq 0, \tag{4.15}$$

where $\varphi_n(t)$ and $\varphi_r(t)$ are deterministic functions defined by the parameter vectors $\{a_n, b_n, \sigma_n, r_n^{\mathbb{Q}}(0)\}$ and $\{a_r, b_r, \sigma_r, r_r^{\mathbb{Q}}(0)\}$ respectively. These functions, as described in Brigo and Mercurio (2006), are free to have whatever value we choose as long as

$$\varphi_n(0) = r_n^{Cal,\mathbb{Q}}(0) - r_n^{\mathbb{Q}}(0),$$
$$\varphi_r(0) = r_r^{Cal,\mathbb{Q}}(0) - r_r^{\mathbb{Q}}(0).$$

Through equations 4.14 and 4.15 and an application of Itô's lemma, we can write the risk-neutral dynamics of $r_n^{Cal,\mathbb{Q}}(t)$ and $r_r^{Cal,\mathbb{Q}}(t)$ as:

$$dr_n^{Cal,\mathbb{Q}}(t) = \left[b_n + a_n\varphi_n(t) + \frac{d\varphi_n(t)}{dt} - a_n r_n^{Cal,\mathbb{Q}}(t)\right]\ dt + \sigma_n\, dW_n^{\mathbb{Q}}(t),$$
$$dr_r^{Cal,\mathbb{Q}}(t) = \left[b_r - \rho_{rI}\sigma_I\sigma_r + a_r\varphi_r(t) + \frac{d\varphi_r(t)}{dt} - a_r r_r^{Cal,\mathbb{Q}}(t)\right]\ dt + \sigma_r\, dW_r^{\mathbb{Q}}(t)$$

Now, Brigo and Mercurio (2006) show that the models above will fit the currently observed term structure of discount factors if and only if:

$$\varphi_n(t) := f_n^{Obs}(0,t) - f_n(0,t),$$
$$\varphi_r(t) := f_r^{Obs}(0,t) - f_r(0,t),$$

where $f_n^{Obs}(0,t)$ and $f_n^{Obs}(0,t)$ are the currently observed instantaneous forward rates. Moreover, under the Vasiček model specification, Brigo and Mercurio (2006) show that we can define $\varphi_n(t)$ and $\varphi_r(t)$ as:

$$\varphi_n(t) = f_n^{Obs}(0,t) - \left(1 - e^{-a_n t}\right)\left(\frac{a_n b_n - \frac{1}{2}\sigma_n^2}{a_n^2} + \frac{\sigma_n^2}{2a_n^2}e^{-a_n t}\right) - r_n^{\mathbb{Q}}(0)e^{-a_n t},$$

$$\varphi_r(t) = f_r^{Obs}(0,t) - \left(1 - e^{-a_r t}\right)\left(\frac{a_r(b_r - \rho_{rI}\sigma_I\sigma_r) - \frac{1}{2}\sigma_r^2}{a_r^2} + \frac{\sigma_r^2}{2a_r^2}e^{-a_r t}\right) - r_r^{\mathbb{Q}}(0)e^{-a_r t}.$$

This choice of $\varphi_n(t)$ and $\varphi_r(t)$ ensures that the model for $r_n^{Cal,\mathbb{Q}}(t)$ and $r_r^{Cal,\mathbb{Q}}(t)$ will exactly fit the observed term structure of interest rates, regardless of the values of $\{a_n, b_n, \sigma_n, r_n^{\mathbb{Q}}(0)\}$ and $\{a_r, b_r, \sigma_r, r_r^{\mathbb{Q}}(0)\}$ that are chosen. Importantly, Brigo and Mercurio (2006) also give an explicit formula for the pricing of zero-coupon bonds under the calibrated model:

$$P_n^{Cal}(t,T) = \frac{P_n^{Obs}(0,T)e^{C_n(0,t) - D_n(0,t)r_n^{\mathbb{Q}}(0)}}{P_n^{Obs}(0,t)e^{C_n(0,T) - D_n(0,T)r_n^{\mathbb{Q}}(0)}} e^{C_n(t,T) - D_n(t,T)\left[r_n^{Cal,\mathbb{Q}}(t) - \varphi_n(t)\right]}, \quad (4.16)$$

$$P_r^{Cal}(t,T) = \frac{P_r^{Obs}(0,T)e^{C_r(0,t) - D_r(0,t)r_r^{\mathbb{Q}}(0)}}{P_r^{Obs}(0,t)e^{C_r(0,T) - D_r(0,T)r_r^{\mathbb{Q}}(0)}} e^{C_r(t,T) - D_r(t,T)\left[r_r^{Cal,\mathbb{Q}}(t) - \varphi_r(t)\right]}, \quad (4.17)$$

where $C_n(t,T)$, $C_r(t,T)$, $D_n(t,T)$ and $D_r(t,T)$ are as defined in sections 3.2.1 and 3.3.1. Note that the quantities $r_n^{Cal,\mathbb{Q}}(t) - \varphi_n(t)$ and $r_r^{Cal,\mathbb{Q}}(t) - \varphi_r(t)$ can be replaced by $r_n^{\mathbb{Q}}(t)$ and $r_r^{\mathbb{Q}}(t)$ respectively, by equations 4.14 and 4.15. This then allows us to price zero-coupon bonds under the calibrated model such that they are consistent with the observable nominal and real zero-coupon bonds in the market, by only having to simulate values for $r_n^{\mathbb{Q}}(t)$ and $r_r^{\mathbb{Q}}(t)$ under the risk-neutral measure. This is easily done by employing the simulation method discussed in Chapter 3, and setting λ_n, λ_r and λ_I all equal to 0.

4.5.2 Simulation Under the Calibrated Model

As discussed in the previous section, in order to price and recover the observed nominal and real zero-coupon bonds, we are only required to simulate under the risk-neutral measure. Thus, our model is completely defined by:

$$\begin{aligned}
dr_n^{\mathbb{Q}}(t) &= \left[b_n - a_n r_n^{\mathbb{Q}}(t)\right]\, dt + \sigma_n\, dW_n^{\mathbb{Q}}(t) \\
dr_r^{\mathbb{Q}}(t) &= \left[b_r - \rho_{rI}\sigma_I\sigma_r - a_r r_r^{\mathbb{Q}}(t)\right]\, dt + \sigma_r\, dW_r^{\mathbb{Q}}(t) \\
\frac{dI^{\mathbb{Q}}(t)}{I^{\mathbb{Q}}(t)} &= \left[r_n^{\mathbb{Q}}(t) - r_r^{\mathbb{Q}}(t)\right]\, dt + \sigma_I\, dW_I^{\mathbb{Q}}(t)
\end{aligned}$$

Once the risk-neutral quantities have been simulated, we can deterministically shift each using $\varphi_n(t)$ and $\varphi_r(t)$. For $r_n^{Cal,\mathbb{Q}}(t)$ and $r_r^{Cal,\mathbb{Q}}(t)$, the matter is quite trivial, we

just employ equations (4.14) and (4.15). For $I^{Cal,\mathbb{Q}}(t)$ however, we will need to do some manipulation. In Appendix C.2 we show that we can write $I^{Cal,\mathbb{Q}}(t_i)|\mathcal{F}_{t_{i-1}}$ as follows:

$$I^{Cal,\mathbb{Q}}(t_i) = \frac{I^{Cal,\mathbb{Q}}(t_{i-1})I^{\mathbb{Q}}(t_i)}{I^{\mathbb{Q}}(t_{i-1})} e^{\varphi_n(t_{i-1})-\varphi_r(t_{i-1})}. \tag{4.18}$$

Since we will have already simulated $I^{\mathbb{Q}}(t)$ for all discretised t, we can iterate over this expression to calculate $I^{Cal,\mathbb{Q}}(t)$ for all required t too. All that is left is to evaluate $\varphi_n(t)$ and $\varphi_r(t)$, which requires the quantities $f_n^{Obs}(0,t)$ and $f_r^{Obs}(0,t)$. Since we do not have data for the instantaneous forward rates, we will employ the following discretisation:

$$P_n^{Obs}(0,T_j) = \exp\left[-\sum_{j=1}^{M-1} f_n^{Obs}(0,T_j)(T_{j+1}-T_j)\right],$$
$$P_r^{Obs}(0,T_j) = \exp\left[-\sum_{j=1}^{M-1} f_r^{Obs}(0,T_j)(T_{j+1}-T_j)\right],$$

which allows us to write $f_n^{Obs}(0,T_j)$ and $f_r^{Obs}(0,T_j)$ for $j \in \{0,1,...,M-1\}$ (we define $T_0 := 0$) as follows:

$$f_n^{Obs}(0,T_j) = -\frac{\ln\left(P_n^{Obs}(0,T_{j+1})/P_n^{Obs}(0,T_j)\right)}{T_{j+1}-T_j},$$
$$f_r^{Obs}(0,T_j) = -\frac{\ln\left(P_r^{Obs}(0,T_{j+1})/P_r^{Obs}(0,T_j)\right)}{T_{j+1}-T_j}.$$

We will again be simulating over the time horizon $[0,8]$ (to remain consistent with the simulations in Chapter 3 as well as the estimated time horizon in this chapter), specifying 250 trading days per year. Thus we will be simulating $N = 2000$ values. We will again choose 30-Sep-2021 as time 0 (i.e., the current time from which we will take the observed nominal and real zero-coupon bond prices). We will also be making use of the estimated parameters contained in table 4.3 and 4.4 (except for $\hat{\lambda}_n$ and $\hat{\lambda}_r$, as we are working under $\mathbb{Q}$).

We can then use equations (4.16) and (4.17) to simulate both nominal and real zero-coupon bond prices (and hence can also derive the associated yield curves using equation (4.1)) under the calibrated model. In figure 4.5, as a proof of concept, we demonstrate the fact that the calibrated model exactly recovers the observed nominal and real yield curve on 30-Sep-2021.

4.6 Forecasting Inflation Under the Risk-Neutral Measure

In this section, we consider using the calibrated model under the risk-neutral measure $\mathbb{Q}$ to produce a forecast for future break-even inflation and realised inflation.

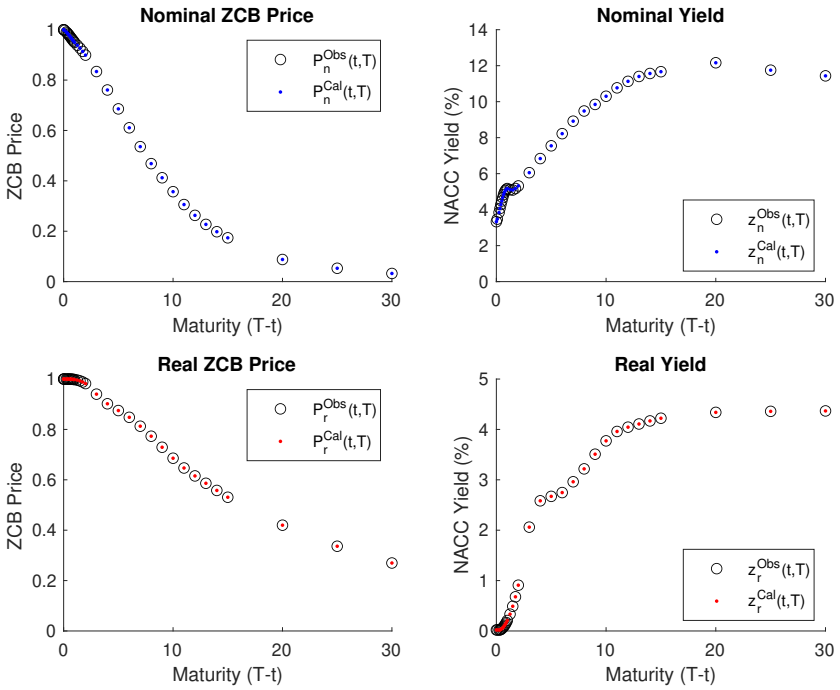

Fig. 4.5: Observed vs simulated zero-coupon bond prices and yields on 30-Sep-2021 under the calibrated model.

We will also compare to the forecasts generated using the estimated model under the real-world measure $\mathbb{P}$.

4.6.1 Forecasting Break-Even Inflation

Following the exact same approach as with the estimated $\mathbb{P}$-model, we simulate 1000 sample paths of $r_n^{Cal,\mathbb{Q}}$ and $r_r^{Cal,\mathbb{Q}}$ over the time horizon $[0, 8]$. However, since $\varphi_n(t)$ and $\varphi_r(t)$ are only defined for values of t where there are observable instantaneous forward rates $f_n^{Obs}(0,t)$ and $f_r^{Obs}(0,t)$, we cannot produce values for $r_n^{Cal,\mathbb{Q}}$ and $r_r^{Cal,\mathbb{Q}}$ for each discretised t_i as defined in equation (3.16). This is an area where simulating under the real-world measure $\mathbb{P}$ is preferable, since there is no restriction on the times that values of $r_n(t)$ and $r_r(t)$ can be simulated. Further, because of how $P_n^{Cal}(t,T)$ and $P_r^{Cal}(t,T)$ are defined in equations (4.16) and (4.17), as we move forward in time along the t dimension, we "run out" of maturities T. For example, at time $t = 8$, the T_j that are left are:

$$\{T_{23} = 9,\ T_{24} = 10,\ \cdots,\ T_{28} = 14,\ T_{29} = 15,\ T_{30} = 20,\ T_{31} = 25,\ T_{32} = 30\},$$

which corresponds to times-to-maturity $T_j - t$ of $\{1, 2, ..., 6, 7, 12, 17, 22\}$. Thus, working on the time horizon of $[0, 8]$, we are only able to simulate calibrated zero-coupon prices of a maximum maturity of 7 years if we wish to have constant yearly increments (since we cannot use $T_j \in \{20, 25, 30\}$ unless we were working with constant increments of 5 years). This is another area where the estimated $\mathbb{P}$-model is better suited, as there is no restriction as to the maximum maturity of zero-coupon bond prices that can be simulated. Working on the time dimension of $[0, 8]$ and only generating estimates of $\pi(t; T_j)$ for $T_j \in \{1, 2, 3, 5\}$ ensures that we do not run into any of these problems. As such, we follow the same approach as in section 4.4.2, and display our estimates and 95% confidence intervals for $\pi(t; 1)$, $\pi(t; 2)$, $\pi(t; 3)$ and $\pi(t; 5)$ in figure 4.6. Again, please note that in the figure, $t = 0$ corresponds to 30-Sep-2021.

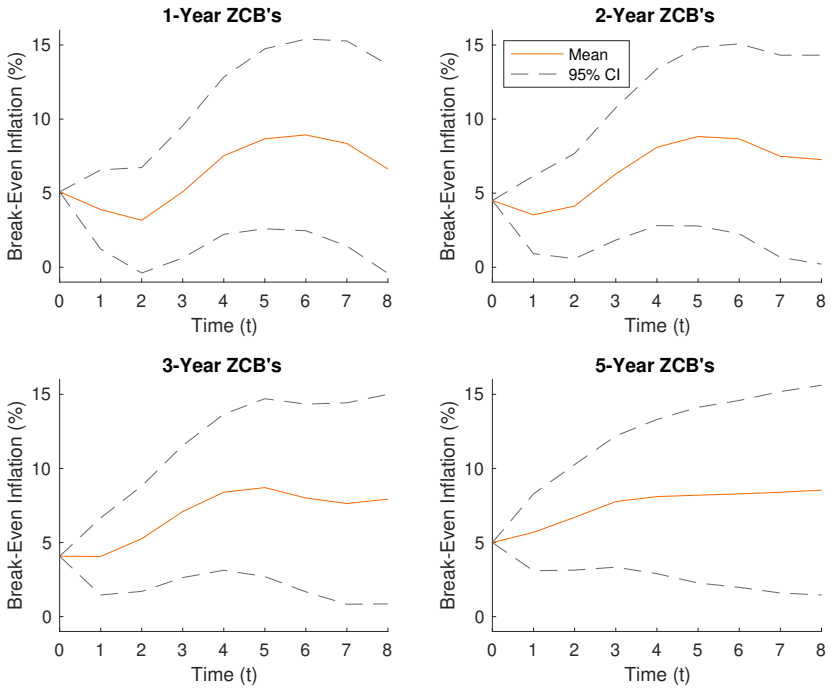

Fig. 4.6: Break-even inflation forecasts inferred from 1-year, 2-year, 3-year and 5-year simulated zero-coupon bonds under the calibrated $\mathbb{Q}$-model.

Note how the curves produced are not as smooth as in the estimated $\mathbb{P}$-model (as we are restricted to working in yearly increments and cannot generate daily estimates as under the real-world measure $\mathbb{P}$). Also note how there is more of a difference in shape between break-even inflation inferred from the different T_j-maturity zero-coupon bond prices in comparison to the estimated $\mathbb{P}$-model, where

the overall shape was the same for each $T_j \in \{1, 2, 3, 5\}$. This is due to the fact that $P_n^{Cal}(t, T)$ and $P_r^{Cal}(t, T)$ are deterministically adjusted based on the observed bond prices at time t, whereas $P_n(t, T)$ and $P_r(t, T)$ under the $\mathbb{P}$-model are purely simulated quantities. That being said, there is still considerable consistency between both the estimated $\mathbb{P}$-model and the calibrated $\mathbb{Q}$-model in that under both models, $\pi(t; T_j)$ increases over time to end up at a yearly break-even inflation estimate of approximately 8% at time $t = 8$ (corresponding to 30-Sep-2029).

4.6.2 Forecasting Realised Inflation

Lastly, since we are able to simulate the CPI process $I^{Cal,\mathbb{Q}}(t)$ under the calibrated $\mathbb{Q}$-model, we are able to also provide an estimate of realised inflation over the period $[0, 8]$. We define annual realised inflation as:

$$\pi_{Realised}(t) := \frac{I^{Cal,\mathbb{Q}}(t) - I^{Cal,\mathbb{Q}}(t-1)}{I^{Cal,\mathbb{Q}}(t-1)}, \quad \text{for } t \in \{1, 2, 3, ..., 8\}.$$

In this case, we interpret $\pi_{Realised}(t)$ as the annual realised inflation over year t (i.e., from time $t-1$ to t). We use the same 1000 simulated sample paths as used in forecasting break-even inflation, except this time we only use $I^{Cal,\mathbb{Q}}(t)$, and follow the same procedure of taking the mean and standard deviation to generate estimates and confidence intervals for $\pi_{Realised}(t)$ over $[0, 8]$, which we display in figure 4.7. Again, please note that in the figure, $t = 0$ corresponds to 30-Sep-2021.

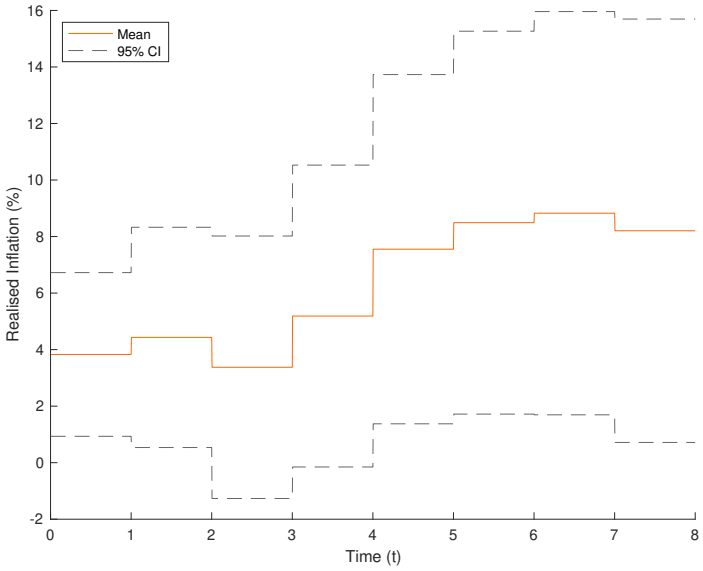

Fig. 4.7: Realised inflation forecasts under the calibrated $\mathbb{Q}$-model.

Notice how the annual realised inflation curve mimics the shapes of the inferred break-even inflation curves under the $\mathbb{Q}$-model, and how, like under both $\mathbb{P}$- and $\mathbb{Q}$-models, it exhibits an increasing trend over time to end up at approximately 8% at time $t = 8$ (corresponding to 30-Sep-2029).

Chapter 5

Conclusion

In this dissertation we have developed a three-factor model under the HJM framework following the work done by Jarrow and Yildirim (2003). We have shown how the model can be used to jointly simulate the nominal short rates, real short rates and the CPI using theoretical parameters, and how it can then be used to price nominal and real zero-coupon bonds within the model. We then demonstrated how the Kalman filter algorithm as described in Bolder (2001) can be applied to estimate these model parameters using observed bond data, and applied this estimation procedure to South African government bond data. It was found that the Kalman filter was not able to fit the nominal and real yield curve data well for long-term bond maturities, and it is suggested that for future research a multi-factor nominal and real short rate process should be considered so as to better capture the true underlying dynamics of the observed yield curve. Using these estimated parameters, we were then able to produce a forecast of break-even inflation under the real-world measure $\mathbb{P}$, which displayed an increasing trend over the considered time horizon. Lastly, we applied the general deterministic-shift extension as described by Brigo and Mercurio (2006) for time-homogeneous short rate models to the nominal and real short rate processes in order to produce a calibrated model under the risk-neutral measure $\mathbb{Q}$ that is able to exactly recover the initial observed nominal and real term structure. For comparison to the estimated $\mathbb{P}$-model, we then produced forecasts of break-even and realised inflation under the risk-neutral measure $\mathbb{Q}$ and found that the overall increasing trend over the considered time horizon was the same.

Overall, this dissertation has presented an introduction to modelling the South African inflation bond market; while there have been areas where we have suggested improvements for future research, we have still been able to produce both a real-world estimated $\mathbb{P}$-model and a risk-neutral calibrated $\mathbb{Q}$-model that can both be used to price nominal and real zero-coupon bonds, as well as forecast future inflation values in South Africa.

Bibliography

Babbs, S. and Nowman, K. (1999). Kalman filtering of generalized Vasicek term structure models, *Journal of Financial and Quantitative Analysis* **34**(1): 115–130.

Belgrade, N., Benhamou, E. and Koehler, E. (2004). A market model for inflation, *Cahiers de la Maison des Sciences Economiques* .

Björk, T. (2009). *Arbitrage Theory in Continuous Time*, 3 edn, Oxford University Press.

Bolder, D. (2001). Affine term-structure models: theory and implementation, *Bank of Canada Working Paper No. 2001-15* .

Brigo, D. and Mercurio, F. (2006). *Interest rate models-theory and practice: with smile, inflation and credit*, Vol. 2, Berlin: Springer.

Dam, H. T., Macrina, A., Skovmand, D. and Sloth, D. (2020). Rational models for inflation-linked derivatives, *SIAM Journal on Financial Mathematics* **11**(4): 974–1006.

De Jong, F. (2000). Time series and cross-section information in affine term-structure models, *Journal of Business & Economic Statistics* **18**(3): 300–314.

Duan, J. and Simonato, J. (1999). Estimating and testing exponential-affine term structure models by Kalman filter, *Review of Quantitative Finance and Accounting* **13**(2): 111–135.

Duffee, G. R. and Stanton, R. H. (2012). Estimation of dynamic term structure models., *The Quarterly Journal of Finance* **2**(02): 1250008.

Heath, D., Jarrow, R. and Morton, A. (1992). Bond pricing and the term structure of interest rates: a new methodology for contingent claims valuation, *Econometrica* **60**(1): 77–105.

Jarrow, R. and Turnbull, S. (1998). A unified approach for pricing contingent claims on multiple term structures, *Review of Quantitative Finance and Accounting* **10**(1): 5–19.

Jarrow, R. and Yildirim, Y. (2003). Pricing treasury inflation protected securities and related derivatives using an HJM model, *Journal of Financial and Quantitative Analysis* **38**(2): 337–358.

Kalman, R. (1960). A new approach to linear filtering and prediction problems, *Transactions of the ASME–Journal of Basic Engineering* **82**(Series D): 35–45.

Mercurio, F. (2005). Pricing inflation-indexed derivatives, *Quantitative Finance* **5**(3): 289–302.

Mercurio, F. and Moreni, N. (2005). Pricing inflation-indexed options with stochastic volatility, *Product and Business Development Group, Banca Imi, San Paolo Imi Group* .

Raffaelli, M. (2007). Pricing methodology for inflation indexed bonds, *Bond Exchange of South Africa (BESA)* .

Vasiček, O. (1977). An equilibrium characterization of the term structure, *Journal of Financial Economics* **5**(2): 177–188.

Welch, G. and Bishop, G. (1995). An introduction to the Kalman filter, *Chapel Hill, NC, USA* .

Appendix A

Chapter 2 Proofs

A.1 Arbitrage-Free Drift Conditions Proofs

A.1.1 Proof of Equation (2.5)

From equation (2.1), we have:

$$df_n(t,T) = \alpha_n(t,T)\,dt + \sigma_n(t,T)\,dW_n^{\mathbb{P}}(t),$$

thus we can write:

$$\begin{aligned} df_n(u,s) &= \alpha_n(u,s)\,du + \sigma_n(u,s)\,dW_n^{\mathbb{P}}(u), \\ \therefore f_n(t,s) - f_n(0,s) &= \int_0^t \alpha_n(u,s)\,du + \int_0^t \sigma_n(u,s)\,dW_n^{\mathbb{P}}(u), \\ \therefore f_n(t,s) &= f_n(0,s) + \int_0^t \alpha_n(u,s)\,du + \int_0^t \sigma_n(u,s)\,dW_n^{\mathbb{P}}(u). \end{aligned}$$

Now we define $Y_n(t,T) := -\int_t^T f_n(t,s)\,ds$ such that $P_n(t,T) = e^{-\int_t^T f_n(t,s)\,ds} = e^{Y_n(t,T)}$. From the definition of $f_n(t,s)$ above, we can write:

$$\begin{aligned} Y_n(t,T) &= -\int_t^T f_n(t,s)\,ds \\ &= -\underbrace{\int_t^T f_n(0,s)\,ds}_{(1)} - \underbrace{\int_t^T \int_0^t \alpha_n(u,s)\,du\,ds}_{(2)} - \underbrace{\int_t^T \int_0^t \sigma_n(u,s)\,dW_n^{\mathbb{P}}(u)\,ds}_{(3)}. \end{aligned}$$

Manipulating (1):

$$\begin{aligned} \int_t^T f_n(0,s)\,ds &= \int_0^T f_n(0,s)\,ds - \int_0^t f_n(0,s)\,ds \\ &= -Y_n(0,T) - \int_0^t f_n(0,s)\,ds. \end{aligned}$$

Manipulating (2), using the Fubini theorem (see Björk (2009)):

$$\begin{aligned}\int_t^T \int_0^t \alpha_n(u,s)\,du\,ds &= \int_0^t \int_t^T \alpha_n(u,s)\,ds\,du \\ &= \int_0^t \int_u^T \alpha_n(u,s)\,ds\,du - \int_0^t \int_u^t \alpha_n(u,s)\,ds\,du \\ &= \int_0^t \int_u^T \alpha_n(u,s)\,ds\,du - \int_0^t \int_0^s \alpha_n(u,s)\,du\,ds.\end{aligned}$$

In the same way, manipulating (3):

$$\int_t^T \int_0^t \sigma_n(u,s)\,dW_n^{\mathbb{P}}(u)\,ds = \int_0^t \int_u^T \sigma_n(u,s)\,ds\,dW_n^{\mathbb{P}}(u) - \int_0^t \int_0^s \sigma_n(u,s)\,dW_n^{\mathbb{P}}(u)\,ds.$$

Thus we can put all (1), (2), (3) together to write $Y_n(t,T)$ as follows:

$$\begin{aligned}Y_n(t,T) &= Y_n(0,T) - \int_0^t \int_u^T \alpha_n(u,s)\,ds\,du - \int_0^t \int_u^T \sigma_n(u,s)\,ds\,dW_n^{\mathbb{P}}(u) \\ &\quad + \int_0^t f_n(0,s)\,ds + \int_0^t \int_0^s \alpha_n(u,s)\,du\,ds + \int_0^t \int_0^s \sigma_n(u,s)\,dW_n^{\mathbb{P}}(u)\,ds \\ &= Y_n(0,T) - \int_0^t \int_u^T \alpha_n(u,s)\,ds\,du - \int_0^t \int_u^T \sigma_n(u,s)\,ds\,dW_n^{\mathbb{P}}(u) \\ &\quad + \int_0^t \underbrace{\left(f_n(0,s) + \int_0^s \alpha_n(u,s)\,du + \int_0^s \sigma_n(u,s)\,dW_n^{\mathbb{P}}(u)\right)}_{=f_n(s,s)=r_n(s)}\,ds.\end{aligned}$$

Thus we can write $dY_n(t,T)$ as:

$$dY_n(t,T) = \left(r_n(t) - \int_t^T \alpha_n(t,s)\,ds\right)dt - \left(\int_t^T \sigma_n(t,s)\,ds\right)dW_n^{\mathbb{P}}(t).$$

Applying Itô's lemma as described in Björk (2009) to $P_n(t,T) = e^{Y_n(t,T)}$, we obtain the following:

$$\begin{aligned}dP_n(t,T) &= P_n(t,T)\,dY_n(t,T) + \tfrac{1}{2}P_n(t,T)\big(dY_n(t,T)\big)^2, \\ \therefore \frac{dP_n(t,T)}{P_n(t,T)} &= \left(r_n(t) - \int_t^T \alpha_n(t,s)\,ds + \frac{1}{2}\left(\int_t^T \sigma_n(t,s)\,ds\right)^2\right)dt \\ &\quad - \left(\int_t^T \sigma_n(t,s)\,ds\right)dW_n^{\mathbb{P}}(t).\end{aligned}$$

So now we have the $\mathbb{P}$-dynamics of $P_n(t,T)$. However, we want to look at the dynamics of $\frac{P_n(t,T)}{B_n(t)}$, which we can use Itô's lemma to find. Note first that by our definition of $B_n(t)$, we have:

$$\begin{aligned}B_n(t) &= e^{\int_0^t r_n(s)\,ds}, \\ \therefore dB_n(t) &= r_n(t)e^{\int_0^t r_n(s)\,ds}\,dt = r_n(t)B_n(t)\,dt.\end{aligned}$$

Now we can apply Itô to $\frac{P_n(t,T)}{B_n(t)}$:

$$\begin{aligned}
d\left(\frac{P_n(t,T)}{B_n(t)}\right) &= \frac{1}{B_n(t)}\,dP_n(t,T) - \frac{P_n(t,T)}{B_n(t)^2}dB_n(t) \\
&\quad + \frac{1}{2}\left(0 + 2\left(-\frac{1}{B_n(t)^2}\right)\underbrace{dP_n(t,T)dB_n(t)}_{=0} + \frac{P_n(t,T)}{B_n(t)^3}\underbrace{\big(dB_n(t)\big)^2}_{=0}\right) \\
&= \frac{P_n(t,T)}{B_n(t)}\left(r_n(t) - \int_t^T \alpha_n(t,s)\,ds + \frac{1}{2}\left(\int_t^T \sigma_n(t,s)\,ds\right)^2\right)dt \\
&\quad - \frac{P_n(t,T)}{B_n(t)}\left(\int_t^T \sigma_n(t,s)\,ds\right)dW_n^{\mathbb{P}}(t) \\
&\quad - \frac{P_n(t,T)}{B_n(t)}r_n(t)\,dt \\
&= \frac{P_n(t,T)}{B_n(t)}\left(-\int_t^T \alpha_n(t,s)\,ds + \frac{1}{2}\left(\int_t^T \sigma_n(t,s)\,ds\right)^2\right)dt \\
&\quad - \frac{P_n(t,T)}{B_n(t)}\left(\int_t^T \sigma_n(t,s)\,ds\right)dW_n^{\mathbb{P}}(t).
\end{aligned}$$

Now, by Girsanov's theorem (see equation (2.4)):

$$\begin{aligned}
dW_n^{\mathbb{Q}}(t) &= dW_n^{\mathbb{P}}(t) - \lambda_n(t)\,dt, \\
\therefore dW_n^{\mathbb{P}}(t) &= dW_n^{\mathbb{Q}}(t) + \lambda_n(t)\,dt.
\end{aligned}$$

Thus, we have:

$$\begin{aligned}
d\left(\frac{P_n(t,T)}{B_n(t)}\right) = \frac{P_n(t,T)}{B_n(t)}\Bigg(&-\int_t^T \alpha_n(t,s)\,ds + \frac{1}{2}\left(\int_t^T \sigma_n(t,s)\,ds\right)^2 \\
&- \lambda_n(t)\int_t^T \sigma_n(t,s)\,ds\Bigg)dt \\
&- \frac{P_n(t,T)}{B_n(t)}\left(\int_t^T \sigma_n(t,s)\,ds\right)dW_n^{\mathbb{Q}}(t).
\end{aligned}$$

Now, we require $\frac{P_n(t,T)}{B_n(t)}$ to be a $\mathbb{Q}$-martingale, i.e., the process must be driftless:

$$-\int_t^T \alpha_n(t,s)\,ds + \frac{1}{2}\left(\int_t^T \sigma_n(t,s)\,ds\right)^2 - \lambda_n(t)\int_t^T \sigma_n(t,s)\,ds = 0.$$

Differentiating this equation with respect to T yields the following:

$$-\alpha_n(t,T) + \sigma_n(t,T)\int_t^T \sigma_n(t,s)\,ds - \lambda_n(t)\sigma_n(t,T) = 0.$$

And thus we arrive at equation (2.5):

$$\alpha_n(t,T) = \sigma_n(t,T)\left(\int_t^T \sigma_n(t,s)\,ds - \lambda_n(t)\right).$$

A.1.2 Proof of Equation (2.6)

From equation (2.2), we have:

$$df_r(t,T) = \alpha_r(t,T)\,dt + \sigma_r(t,T)\,dW_r^{\mathbb{P}}(t).$$

Following the same method as in the proof of equation (2.5), we can find the $\mathbb{P}$-dynamics of $P_r(t,T)$:

$$\frac{dP_r(t,T)}{P_r(t,T)} = \left(r_r(t) - \int_t^T \alpha_r(t,s)\,ds + \frac{1}{2}\left(\int_t^T \sigma_r(t,s)\,ds\right)^2\right)dt - \left(\int_t^T \sigma_r(t,s)\,ds\right)dW_r^{\mathbb{P}}(t).$$

Now, we would like to find the dynamics of $\frac{I(t)P_r(t,T)}{B_n(t)}$, so we can again use Itô's lemma:

$$\begin{aligned}
d\left(\frac{I(t)P_r(t,T)}{B_n(t)}\right) &= \frac{P_r(t,T)}{B_n(t)}\,dI(t) + \frac{I(t)}{B_n(t)}\,dP_r(t,T) - \frac{I(t)P_r(t,T)}{B_n(t)^2}\,dB_n(t) \\
&\quad + \frac{1}{2}\Bigg(0 + 0 + 2\frac{1}{B_n(t)}\,dI(t)\,dP_r(t,T) - 2\frac{P_r(t,T)}{B_n(t)^2}\underbrace{dI(t)\,dB_n(t)}_{=0} \\
&\qquad - 2\frac{I(t)}{B_n(t)^2}\underbrace{dP_r(t,T)\,dB_n(t,T)}_{=0} + 2\frac{I(t)P_r(t,T)}{B_n(t)^2}\underbrace{\big(dB_n(t)\big)^2}_{=0}\Bigg) \\
&= \frac{I(t)P_r(t,T)}{B_n(t)}\big(\mu_I(t)\,dt + \sigma_I(t)\,dW_I^{\mathbb{P}}(t)\big) \\
&\quad + \frac{I(t)P_r(t,T)}{B_n(t)}\left(r_r(t) - \int_t^T \alpha_r(t,s)\,ds + \frac{1}{2}\left(\int_t^T \sigma_r(t,s)\,ds\right)^2\right)dt \\
&\quad - \frac{I(t)P_r(t,T)}{B_n(t)}\left(\int_t^T \sigma_r(t,s)\,ds\right)dW_r^{\mathbb{P}}(t) \\
&\quad - \frac{I(t)P_r(t,T)}{B_n(t)}r_n(t)\,dt \\
&\quad - \frac{I(t)P_r(t,T)}{B_n(t)}\sigma_I(t)\left(\int_t^T \sigma_r(t,s)\,ds\right)\underbrace{dW_I^{\mathbb{P}}(t)\,dW_r^{\mathbb{P}}(t)}_{=\rho_{rI}\,dt} \\
&= \frac{I(t)P_r(t,T)}{B_n(t)}\Bigg(\mu_I(t) + r_r(t) - \int_t^T \alpha_r(t,s)\,ds + \frac{1}{2}\left(\int_t^T \sigma_r(t,s)\,ds\right)^2 \\
&\qquad - r_n(t) - \sigma_I(t)\rho_{rI}\int_t^T \sigma_r(t,s)\,ds\Bigg)dt \\
&\quad + \frac{I(t)P_r(t,T)}{B_n(t)}\sigma_I(t)\,dW_I^{\mathbb{P}}(t) \\
&\quad - \frac{I(t)P_r(t,T)}{B_n(t)}\left(\int_t^T \sigma_r(t,s)\,ds\right)dW_r^{\mathbb{P}}(t).
\end{aligned}$$

By Girsanov's theorem (see equation (2.4)):

$$dW_I^{\mathbb{Q}}(t) = dW_I^{\mathbb{P}}(t) - \lambda_I(t)\,dt, \qquad dW_r^{\mathbb{Q}}(t) = dW_r^{\mathbb{P}}(t) - \lambda_r(t)\,dt,$$
$$\therefore dW_I^{\mathbb{P}}(t) = dW_I^{\mathbb{Q}}(t) + \lambda_I(t)\,dt. \qquad \therefore dW_r^{\mathbb{P}}(t) = dW_r^{\mathbb{Q}}(t) + \lambda_r(t)\,dt.$$

So we have the following $\mathbb{Q}$-dynamics:

$$\begin{aligned} d\left(\frac{I(t)P_r(t,T)}{B_n(t)}\right) = \frac{I(t)P_r(t,T)}{B_n(t)}\Bigg(&\mu_I(t) + r_r(t) - \int_t^T \alpha_r(t,s)\,ds + \frac{1}{2}\left(\int_t^T \sigma_r(t,s)\,ds\right)^2 \\ &- r_n(t) - \sigma_I(t)\rho_{rI}\int_t^T \sigma_r(t,s)\,ds + \lambda_I(t)\sigma_I(t) \\ &- \lambda_r(t)\int_t^T \sigma_r(t,s)\,ds\Bigg)dt \\ &+ \frac{I(t)P_r(t,T)}{B_n(t)}\sigma_I(t)\,dW_I^{\mathbb{Q}}(t) \\ &- \frac{I(t)P_r(t,T)}{B_n(t)}\left(\int_t^T \sigma_r(t,s)\,ds\right)dW_r^{\mathbb{Q}}(t). \end{aligned}$$

For $\frac{I(t)P_r(t,T)}{B_n(t)}$ to be a $\mathbb{Q}$-martingale, we require the above process to be driftless, i.e.,

$$\begin{aligned} 0 = \mu_I(t) - r_n(t) + r_r(t) + \lambda_I(t)\sigma_I(t) - \int_t^T \alpha_r(t,s)\,ds + \frac{1}{2}\left(\int_t^T \sigma_r(t,s)\,ds\right)^2 \\ - \sigma_I(t)\rho_{rI}\int_t^T \sigma_r(t,s)\,ds - \lambda_r(t)\int_t^T \sigma_r(t,s)\,ds. \end{aligned}$$

Note that by the proof of equation (2.7), we have the following definition of $\mu_I(t)$:

$$\mu_I(t) = r_n(t) - r_r(t) - \sigma_I(t)\lambda_I(t),$$

therefore we can write the drift requirement of $\frac{I(t)P_r(t,T)}{B_n(t)}$ as:

$$0 = -\int_t^T \alpha_r(t,s)\,ds + \frac{1}{2}\left(\int_t^T \sigma_r(t,s)\,ds\right)^2 - \sigma_I(t)\rho_{rI}\int_t^T \sigma_r(t,s)\,ds - \lambda_r(t)\int_t^T \sigma_r(t,s)\,ds.$$

Differentiating with respect to T:

$$0 = -\alpha_r(t,T) + \sigma_r(t,T)\int_t^T \sigma_r(t,s)\,ds - \sigma_I(t)\rho_{rI}\sigma_r(t,T) - \lambda_r(t)\sigma_r(t,T).$$

And thus we arrive at equation (2.6):

$$\alpha_r(t,T) = \sigma_r(t,T)\left(\int_t^T \sigma_r(t,s)\,ds - \sigma_I(t)\rho_{rI} - \lambda_r(t)\right).$$

A.1.3 Proof of Equation (2.7)

From equation (2.3), we have:

$$\frac{dI(t)}{I(t)} = \mu_I(t)\,dt + \sigma_I(t)\,dW_I^{\mathbb{P}}(t).$$

Following the same overall strategy as the above two proofs, since we require $\frac{I(t)B_r(t)}{B_n(t)}$ to be a $\mathbb{Q}$-martingale, we must first find the dynamics of $\frac{I(t)B_r(t)}{B_n(t)}$:

$$\begin{aligned}
d\left(\frac{I(t)B_r(t)}{B_n(t)}\right) &= \frac{B_r(t)}{B_n(t)}\,dI(t) + \frac{I(t)}{B_n(t)}\,dB_r(t) - \frac{I(t)B_r(t)}{B_n(t)^2}\,dB_n(t) \\
&\quad + \frac{1}{2}\Bigg(0 + 0 + 2\frac{1}{B_n(t)}\underbrace{dI(t)\,dB_r(t)}_{=0} - 2\frac{B_r(t)}{B_n(t)^2}\underbrace{dI(t)\,dB_n(t)}_{=0} \\
&\qquad - 2\frac{I(t)}{B_n(t)^2}\underbrace{dB_r(t)\,dB_n(t,T)}_{=0} + 2\frac{I(t)B_r(t)}{B_n(t)^2}\underbrace{\big(dB_n(t)\big)^2}_{=0}\Bigg) \\
&= \frac{I(t)B_r(t)}{B_n(t)}\big(\mu_I(t)\,dt + \sigma_I(t)\,dW_I^{\mathbb{P}}(t)\big) \\
&\quad + \frac{I(t)B_r(t)}{B_n(t)}r_r(t)\,dt - \frac{I(t)B_r(t)}{B_n(t)}r_n(t)\,dt \\
&= \frac{I(t)B_r(t)}{B_n(t)}\big(\mu_I(t) + r_r(t) - r_n(t)\big)dt \\
&\quad + \frac{I(t)B_r(t)}{B_n(t)}\sigma_I(t)\,dW_I^{\mathbb{P}}(t).
\end{aligned}$$

By Girsanov's theorem (see equation (2.4)):

$$W_I^{\mathbb{P}}(t) = dW_I^{\mathbb{Q}}(t) + \lambda_I(t)\,dt.$$

Thus we have the following $\mathbb{Q}$-dynamics for $\frac{I(t)B_r(t)}{B_n(t)}$:

$$\begin{aligned}
d\left(\frac{I(t)B_r(t)}{B_n(t)}\right) &= \frac{I(t)B_r(t)}{B_n(t)}\big(\mu_I(t) + r_r(t) - r_n(t) + \sigma_I(t)\lambda_I(t)\big)dt \\
&\quad + \frac{I(t)B_r(t)}{B_n(t)}\sigma_I(t)\,dW_I^{\mathbb{Q}}(t).
\end{aligned}$$

In the same way as before, we require $\frac{I(t)B_r(t)}{B_n(t)}$ to be a $\mathbb{Q}$-martingale and so the above process must be driftless, i.e.,

$$\mu_I(t) + r_r(t) - r_n(t) + \sigma_I(t)\lambda_I(t) = 0.$$

And thus we arrive at equation (2.7):

$$\mu_I(t) = r_n(t) - r_r(t) - \sigma_I(t)\lambda_I(t).$$

A.2 Specification of Volatility Functions Proofs

A.2.1 Proof of Equation (2.13)

By equation (2.8), we have:

$$df_n(t,T) = \underbrace{\sigma_n(t,T)\left[\int_t^T \sigma_n(t,s)\,ds\right]}_{\alpha_n^{\mathbb{Q}}(t,T)}\,dt + \sigma_n(t,T)\,dW_n^{\mathbb{Q}}(t).$$

For ease of notation, we define $\alpha_n^{\mathbb{Q}}(t,T)$ as above. By definition, we have that $r_n(t) = f_n(t,t)$ and thus we can write:

$$r_n(t) = f_n(t,t) = \underbrace{f_n(0,t) + \int_0^t \alpha_n^{\mathbb{Q}}(s,t)\,ds}_{\Theta_n(t)} + \int_0^t \sigma_n(s,t)\,dW_n^{\mathbb{Q}}(s).$$

Substituting in our function $\sigma_n(t,T)$ as defined in equation (2.10), we arrive at the following:

$$r_n(t) = \Theta_n(t) + \int_0^t \sigma_n e^{-a_n(t-s)}\,dW_n^{\mathbb{Q}}(s).$$

Taking the derivative with respect to t:

$$\begin{aligned} dr_n(t) &= \Theta_n'(t)\,dt - a_n\left(\int_0^t \sigma_n e^{-a_n(t-s)}\,dW_n^{\mathbb{Q}}(s)\right)dt + \sigma_n\,dW_n^{\mathbb{Q}}(t) \\ &= \Theta_n'(t)\,dt - a_n\big(r_n(t) - \Theta_n(t)\big)\,dt + \sigma_n\,dW_n^{\mathbb{Q}}(t) \\ &= \big[\Theta_n'(t) + a_n\Theta_n(t) - a_n r_n(t)\big]\,dt + \sigma_n\,dW_n^{\mathbb{Q}}(t) \end{aligned}$$

We now define $b_n(t) := \Theta_n'(t) + a_n\Theta_n(t)$, which leads us exactly to equation (2.13):

$$dr_n(t) = \big[b_n(t) - a_n r_n(t)\big]\,dt + \sigma_n\,dW_n^{\mathbb{Q}}(t).$$

The final part of this proof is to solve for the form of $b_n(t)$. First, we note that:

$$\begin{aligned} \Theta_n(t) &= f_n(0,t) + \int_0^t \alpha_n^{\mathbb{Q}}(s,t)\,ds \\ &= f_n(0,t) + \int_0^t \sigma_n(s,t)\left[\int_s^t \sigma_n(s,u)\,du\right]ds \\ &= f_n(0,t) + \frac{\sigma_n^2}{2a_n^2}\left(1 - e^{-a_n t}\right)^2. \end{aligned}$$

Thus we can write $b_n(t)$ as:

$$\begin{aligned} b_n(t) &= \Theta_n'(t) + a_n\Theta_n(t) \\ &= \frac{\partial f_n(0,t)}{\partial T} + \frac{\sigma_n^2}{a_n^2}\left(1 - e^{-a_n t}\right)\left(-a_n e^{-a_n t}\right) + a_n f_n(0,t) + \frac{\sigma_n^2}{2a_n}\left(1 - e^{-a_n t}\right)^2 \\ &= \frac{\partial f_n(0,t)}{\partial T} + a_n f_n(0,t) + \frac{\sigma_n^2}{2a_n}\left(1 - e^{-2a_n t}\right), \end{aligned}$$

which concludes the proof.

A.2.2 Proof of Equation (2.14)

By equation (2.9), we have:

$$\begin{aligned} df_r(t,T) &= \sigma_r(t,T)\left[\int_t^T \sigma_r(t,s)\,ds - \rho_{rI}\sigma_I(t)\right]\,dt + \sigma_r(t,T)\,dW_r^{\mathbb{Q}}(t) \\ &= \underbrace{\sigma_r(t,T)\left[\int_t^T \sigma_r(t,s)\,ds\right]}_{\alpha_r^{\mathbb{Q}}(t,T)}\,dt - \sigma_r(t,T)\rho_{rI}\sigma_I(t)\,dt + \sigma_r(t,T)\,dW_r^{\mathbb{Q}}(t). \end{aligned}$$

Similarly to the nominal case, we define $\alpha_r^{\mathbb{Q}}(t,T)$ as above. By definition, we have that $r_r(t) = f_r(t,t)$ and thus we can write:

$$r_r(t) = \underbrace{f_r(0,t) + \int_0^t \alpha_r^{\mathbb{Q}}(s,t)\,ds}_{\Theta_r(t)} - \int_0^t \sigma_r(s,t)\rho_{rI}\sigma_I(s)\,ds + \int_0^t \sigma_r(s,t)\,dW_r^{\mathbb{Q}}(s).$$

Substituting in our functions $\sigma_r(t,T)$ and $\sigma_I(t)$ as defined in equations (2.11) and (2.12) respectively, we arrive at the following:

$$r_r(t) = \Theta_r(t) - \int_0^t \sigma_r e^{-a_r(t-s)}\rho_{rI}\sigma_I\,ds + \int_0^t \sigma_r e^{-a_r(t-s)}\,dW_r^{\mathbb{Q}}(s).$$

We then take the derivative with respect to t:

$$\begin{aligned} dr_r(t) &= \Theta_r'(t)\,dt - a_r\left(-\int_0^t \sigma_r e^{-a_r(t-s)}\rho_{rI}\sigma_I\,ds\right) - \rho_{rI}\sigma_I\sigma_r\,dt \\ &\qquad - a_r\left(\int_0^t \sigma_r e^{-a_r(t-s)}\,dW_r^{\mathbb{Q}}(s)\right)dt + \sigma_r\,dW_r^{\mathbb{Q}}(t) \\ &= \Theta_r'(t)\,dt - a_r\big(r_r(t) - \Theta_r(t)\big)\,dt - \rho_{rI}\sigma_I\sigma_r\,dt + \sigma_r\,dW_r^{\mathbb{Q}}(t) \\ &= \big[\Theta_r'(t) + a_r\Theta_r(t) - \rho_{rI}\sigma_I\sigma_r - a_r r_r(t)\big]\,dt + \sigma_r\,dW_r^{\mathbb{Q}}(t) \end{aligned}$$

We now define $b_r(t) := \Theta_r'(t) + a_r\Theta_r(t)$, which leads us exactly to equation (2.14):

$$dr_r(t) = \big[b_r(t) - \rho_{rI}\sigma_I\sigma_r - a_r r_r(t)\big]\,dt + \sigma_r\,dW_r^{\mathbb{Q}}(t).$$

To solve for $b_r(t)$, we follow the exact same process as in the proof of equation (2.13) to arrive at:

$$b_r(t) = \frac{\partial f_r(0,t)}{\partial T} + a_r f_r(0,t) + \frac{\sigma_r^2}{2a_r}\left(1 - e^{-2a_r t}\right).$$

A.3 An Equivalent Representation of the Short Rate Model Proofs

A.3.1 Proof of Equation (2.21)

Beginning directly with the requirement that $dr_n(t)$ must be equal under both representations, we have:

$$\begin{aligned}
\sigma_n \, dW_n^{\mathbb{Q}}(t) &= \tilde{\Sigma}_1 \, d\tilde{W}^{\mathbb{Q}}(t) \\
\sigma_n \, dW_n^{\mathbb{Q}}(t) &= \tilde{\sigma}_{11} \, d\tilde{W}_1^{\mathbb{Q}}(t) + \tilde{\sigma}_{12} \, d\tilde{W}_2^{\mathbb{Q}}(t) + \tilde{\sigma}_{13} \, d\tilde{W}_3^{\mathbb{Q}}(t) \\
\left(\sigma_n \, dW_n^{\mathbb{Q}}(t)\right)^2 &= \left(\tilde{\sigma}_{11} \, d\tilde{W}_1^{\mathbb{Q}}(t) + \tilde{\sigma}_{12} \, d\tilde{W}_2^{\mathbb{Q}}(t) + \tilde{\sigma}_{13} \, d\tilde{W}_3^{\mathbb{Q}}(t)\right)^2 \\
\sigma_n^2 \, dt &= \tilde{\sigma}_{11}^2 \, dt + \tilde{\sigma}_{12}^2 \, dt + \tilde{\sigma}_{13}^2 \, dt \\
\therefore \sigma_n &= \|\tilde{\Sigma}_1\|.
\end{aligned}$$

A.3.2 Proof of Equation (2.22)

In the same manner as in the nominal case, we have:

$$\begin{aligned}
\sigma_r \, dW_r^{\mathbb{Q}}(t) &= \tilde{\Sigma}_2 \, d\tilde{W}^{\mathbb{Q}}(t) \\
&\vdots \\
\therefore \sigma_r &= \|\tilde{\Sigma}_2\|.
\end{aligned}$$

A.3.3 Proof of Equation (2.23)

In the same manner as in the nominal and the real case, we have:

$$\begin{aligned}
\sigma_I \, dW_I^{\mathbb{Q}}(t) &= \tilde{\Sigma}_3 \, d\tilde{W}^{\mathbb{Q}}(t) \\
&\vdots \\
\therefore \sigma_I &= \|\tilde{\Sigma}_3\|.
\end{aligned}$$

A.3.4 Proof of Equation (2.24)

Similar to the above cases, we require that $dr_n(t)dr_r(t)$ is equal under both representations:

$$\begin{aligned}
dr_n(t)dr_r(t) &= dr_n(t)dr_r(t) \\
\left(\sigma_n \, dW_n^{\mathbb{Q}}(t)\right)\left(\sigma_r \, dW_r^{\mathbb{Q}}(t)\right) &= \left(\tilde{\Sigma}_1 \, d\tilde{W}^{\mathbb{Q}}(t)\right)\left(\tilde{\Sigma}_2 \, d\tilde{W}^{\mathbb{Q}}(t)\right) \\
\sigma_n\sigma_r \, dW_n^{\mathbb{Q}}(t)dW_r^{\mathbb{Q}}(t) &= \left(\tilde{\sigma}_{11} \, d\tilde{W}_1^{\mathbb{Q}}(t) + \tilde{\sigma}_{12} \, d\tilde{W}_2^{\mathbb{Q}}(t) + \tilde{\sigma}_{13} \, d\tilde{W}_3^{\mathbb{Q}}(t)\right) \\
&\quad \times \left(\tilde{\sigma}_{21} \, d\tilde{W}_1^{\mathbb{Q}}(t) + \tilde{\sigma}_{22} \, d\tilde{W}_2^{\mathbb{Q}}(t) + \tilde{\sigma}_{23} \, d\tilde{W}_3^{\mathbb{Q}}(t)\right) \\
\sigma_n\sigma_r\rho_{nr} \, dt &= \tilde{\Sigma}_1 \cdot \tilde{\Sigma}_2 \, dt \\
\therefore \rho_{nr} &= \frac{\tilde{\Sigma}_1 \cdot \tilde{\Sigma}_2}{\|\tilde{\Sigma}_1\| \times \|\tilde{\Sigma}_2\|}.
\end{aligned}$$

A.3.5 Proof of Equation (2.25)

In the same way, we require that $dr_n(t)dI(t)$ is equal under both representations:

$$\begin{aligned}
dr_n(t)dI(t) &= dr_n(t)dI(t) \\
\big(\sigma_n\, dW_n^{\mathbb{Q}}(t)\big)\big(I(t)\sigma_I\, dW_I^{\mathbb{Q}}(t)\big) &= \big(\tilde{\Sigma}_1\, d\tilde{W}^{\mathbb{Q}}(t)\big)\big(I(t)\tilde{\Sigma}_3\, d\tilde{W}^{\mathbb{Q}}(t)\big) \\
\sigma_n\sigma_I\, dW_n^{\mathbb{Q}}(t)dW_I^{\mathbb{Q}}(t) &= \big(\tilde{\sigma}_{11}\, d\tilde{W}_1^{\mathbb{Q}}(t) + \tilde{\sigma}_{12}\, d\tilde{W}_2^{\mathbb{Q}}(t) + \tilde{\sigma}_{13}\, d\tilde{W}_3^{\mathbb{Q}}(t)\big) \\
&\quad \times \big(\tilde{\sigma}_{31}\, d\tilde{W}_1^{\mathbb{Q}}(t) + \tilde{\sigma}_{32}\, d\tilde{W}_2^{\mathbb{Q}}(t) + \tilde{\sigma}_{33}\, d\tilde{W}_3^{\mathbb{Q}}(t)\big) \\
\sigma_n\sigma_I\rho_{nI}\, dt &= \tilde{\Sigma}_1 \cdot \tilde{\Sigma}_3\, dt \\
\therefore \rho_{nI} &= \frac{\tilde{\Sigma}_1 \cdot \tilde{\Sigma}_3}{\|\tilde{\Sigma}_1\| \times \|\tilde{\Sigma}_3\|}.
\end{aligned}$$

A.3.6 Proof of Equation (2.26)

And similarly, we require $dr_r(t)dI(t)$ to be equal under both representations:

$$\begin{aligned}
dr_r(t)dI(t) &= dr_r(t)dI(t) \\
\big(\sigma_r\, dW_r^{\mathbb{Q}}(t)\big)\big(I(t)\sigma_I\, dW_I^{\mathbb{Q}}(t)\big) &= \big(\tilde{\Sigma}_2\, d\tilde{W}^{\mathbb{Q}}(t)\big)\big(I(t)\tilde{\Sigma}_3\, d\tilde{W}^{\mathbb{Q}}(t)\big) \\
\sigma_r\sigma_I\, dW_r^{\mathbb{Q}}(t)dW_I^{\mathbb{Q}}(t) &= \big(\tilde{\sigma}_{21}\, d\tilde{W}_1^{\mathbb{Q}}(t) + \tilde{\sigma}_{22}\, d\tilde{W}_2^{\mathbb{Q}}(t) + \tilde{\sigma}_{23}\, d\tilde{W}_3^{\mathbb{Q}}(t)\big) \\
&\quad \times \big(\tilde{\sigma}_{31}\, d\tilde{W}_1^{\mathbb{Q}}(t) + \tilde{\sigma}_{32}\, d\tilde{W}_2^{\mathbb{Q}}(t) + \tilde{\sigma}_{33}\, d\tilde{W}_3^{\mathbb{Q}}(t)\big) \\
\sigma_r\sigma_I\rho_{rI}\, dt &= \tilde{\Sigma}_2 \cdot \tilde{\Sigma}_3\, dt \\
\therefore \rho_{rI} &= \frac{\tilde{\Sigma}_2 \cdot \tilde{\Sigma}_3}{\|\tilde{\Sigma}_2\| \times \|\tilde{\Sigma}_3\|}.
\end{aligned}$$

A.3.7 Proof of Equations (2.30), (2.31) and (2.32)

We start with:

$$\begin{aligned}
d\tilde{W}^{\mathbb{Q}}(t) &= d\tilde{W}^{\mathbb{P}}(t) - \tilde{\Lambda}\, dt \\
\tilde{\Sigma}\, d\tilde{W}^{\mathbb{Q}}(t) &= \tilde{\Sigma}\, d\tilde{W}^{\mathbb{P}}(t) - \tilde{\Sigma}\tilde{\Lambda}\, dt \\
\therefore \begin{bmatrix} \tilde{\Sigma}_1\, d\tilde{W}^{\mathbb{Q}}(t) \\ \tilde{\Sigma}_2\, d\tilde{W}^{\mathbb{Q}}(t) \\ \tilde{\Sigma}_3\, d\tilde{W}^{\mathbb{Q}}(t) \end{bmatrix} &= \begin{bmatrix} \tilde{\Sigma}_1\, d\tilde{W}^{\mathbb{P}}(t) \\ \tilde{\Sigma}_2\, d\tilde{W}^{\mathbb{P}}(t) \\ \tilde{\Sigma}_3\, d\tilde{W}^{\mathbb{P}}(t) \end{bmatrix} - \begin{bmatrix} \tilde{\Sigma}_1\tilde{\Lambda} \\ \tilde{\Sigma}_2\tilde{\Lambda} \\ \tilde{\Sigma}_3\tilde{\Lambda} \end{bmatrix} dt.
\end{aligned}$$

Now note that because of the restrictions $\sigma_n = \|\tilde{\Sigma}_1\|$, $\sigma_r = \|\tilde{\Sigma}_2\|$, $\sigma_I = \|\tilde{\Sigma}_3\|$, we can write (see proof of equation (2.21)):

$$\begin{aligned}
\tilde{\Sigma}_1\, d\tilde{W}^{\mathbb{Q}}(t) &= \sigma_n\, dW_n^{\mathbb{Q}}(t), & \therefore \tilde{\Sigma}_1\, d\tilde{W}^{\mathbb{P}}(t) &= \sigma_n\, dW_n^{\mathbb{P}}(t). \\
\tilde{\Sigma}_2\, d\tilde{W}^{\mathbb{Q}}(t) &= \sigma_n\, dW_r^{\mathbb{Q}}(t), & \therefore \tilde{\Sigma}_2\, d\tilde{W}^{\mathbb{P}}(t) &= \sigma_n\, dW_r^{\mathbb{P}}(t). \\
\tilde{\Sigma}_3\, d\tilde{W}^{\mathbb{Q}}(t) &= \sigma_n\, dW_I^{\mathbb{Q}}(t), & \therefore \tilde{\Sigma}_3\, d\tilde{W}^{\mathbb{P}}(t) &= \sigma_n\, dW_I^{\mathbb{P}}(t).
\end{aligned}$$

Thus we have:

$$\begin{bmatrix} \sigma_n\, dW_n^{\mathbb{Q}}(t) \\ \sigma_r\, dW_r^{\mathbb{Q}}(t) \\ \sigma_I\, dW_I^{\mathbb{Q}}(t) \end{bmatrix} = \begin{bmatrix} \sigma_n\, dW_n^{\mathbb{P}}(t) \\ \sigma_r\, dW_r^{\mathbb{P}}(t) \\ \sigma_I\, dW_I^{\mathbb{P}}(t) \end{bmatrix} - \begin{bmatrix} \tilde{\Sigma}_1\tilde{\Lambda} \\ \tilde{\Sigma}_2\tilde{\Lambda} \\ \tilde{\Sigma}_3\tilde{\Lambda} \end{bmatrix} dt.$$

Now we just use the Girsanov equation $dW_x^{\mathbb{Q}}(t) = dW_x^{\mathbb{P}}(t) - \lambda_x \, dt$ for $x \in \{n, r, I\}$ to simplify:

$$\begin{bmatrix} \sigma_n \, dW_n^{\mathbb{P}}(t) \\ \sigma_r \, dW_r^{\mathbb{P}}(t) \\ \sigma_I \, dW_I^{\mathbb{P}}(t) \end{bmatrix} - \begin{bmatrix} \sigma_n \lambda_n \\ \sigma_r \lambda_r \\ \sigma_I \lambda_I \end{bmatrix} dt = \begin{bmatrix} \sigma_n \, dW_n^{\mathbb{P}}(t) \\ \sigma_r \, dW_r^{\mathbb{P}}(t) \\ \sigma_I \, dW_I^{\mathbb{P}}(t) \end{bmatrix} - \begin{bmatrix} \tilde{\Sigma}_1 \tilde{\Lambda} \\ \tilde{\Sigma}_2 \tilde{\Lambda} \\ \tilde{\Sigma}_3 \tilde{\Lambda} \end{bmatrix} dt$$

$$\therefore \begin{bmatrix} \sigma_n \lambda_n \\ \sigma_r \lambda_r \\ \sigma_I \lambda_I \end{bmatrix} = \begin{bmatrix} \tilde{\Sigma}_1 \tilde{\Lambda} \\ \tilde{\Sigma}_2 \tilde{\Lambda} \\ \tilde{\Sigma}_3 \tilde{\Lambda} \end{bmatrix},$$

which concludes the proof.

Appendix B

Chapter 3 Proofs

B.1 Simulation of the CPI Proofs

B.1.1 Proof of Equation (3.7)

Recall from equation (2.29) that the independent $\mathbb{P}$-dynamics of the CPI are as follows:

$$\begin{aligned}\frac{dI(t)}{I(t)} &= \Big[r_n(t) - r_r(t) - \tilde{\Sigma}_3\tilde{\Lambda}\Big]\ dt + \tilde{\Sigma}_3\, d\tilde{W}^{\mathbb{P}}(t) \\ &= \Big[r_n(t) - r_r(t) - \tilde{\Sigma}_3\tilde{\Lambda}\Big]\ dt + \tilde{\sigma}_{31}\, d\tilde{W}_1^{\mathbb{P}}(t) + \tilde{\sigma}_{32}\, d\tilde{W}_2^{\mathbb{P}}(t) + \tilde{\sigma}_{33}\, d\tilde{W}_3^{\mathbb{P}}(t).\end{aligned}$$

Following the approach provided in Björk (2009), we can solve this stochastic differential equation by applying Itô's lemma:

$$\begin{aligned}d\big(\ln I(s)\big) &= \frac{1}{I(s)}\, dI(s) - \frac{1}{2}\frac{1}{I(s)^2}\big(dI(s)\big)^2 \\ &= \Big[r_n(s) - r_r(s) - \tilde{\Sigma}_3\tilde{\Lambda} - \tfrac{1}{2}\big(\tilde{\sigma}_{31}^2 + \tilde{\sigma}_{32}^2 + \tilde{\sigma}_{33}^2\big)\Big]\ ds \\ &\quad + \tilde{\sigma}_{31}\, d\tilde{W}_1^{\mathbb{P}}(s) + \tilde{\sigma}_{32}\, d\tilde{W}_2^{\mathbb{P}}(s) + \tilde{\sigma}_{33}\, d\tilde{W}_3^{\mathbb{P}}(s) \\ &= \Big[r_n(s) - r_r(s) - \tilde{\Sigma}_3\tilde{\Lambda} - \tfrac{1}{2}\|\tilde{\Sigma}_3\|^2\Big]\ ds \\ &\quad + \tilde{\sigma}_{31}\, d\tilde{W}_1^{\mathbb{P}}(s) + \tilde{\sigma}_{32}\, d\tilde{W}_2^{\mathbb{P}}(s) + \tilde{\sigma}_{33}\, d\tilde{W}_3^{\mathbb{P}}(s).\end{aligned}$$

Integrating both sides from t to T:

$$\begin{aligned}\ln I(T) &= \ln I(t) + \int_t^T \Big[r_n(s) - r_r(s) - \tilde{\Sigma}_3\tilde{\Lambda} - \tfrac{1}{2}\|\tilde{\Sigma}_3\|^2\Big]\ ds \\ &\quad + \int_t^T \tilde{\sigma}_{31}\, d\tilde{W}_1^{\mathbb{P}}(s) + \int_t^T \tilde{\sigma}_{32}\, d\tilde{W}_2^{\mathbb{P}}(s) + \int_t^T \tilde{\sigma}_{33}\, d\tilde{W}_3^{\mathbb{P}}(s), \\ \therefore I(T) &= I(t)\exp\Bigg[\int_t^T r_n(s)\, ds - \int_t^T r_r(s)\, ds - \big(\tilde{\Sigma}_3\tilde{\Lambda} + \tfrac{1}{2}\|\tilde{\Sigma}_3\|^2\big)(T-t) \\ &\quad + \tilde{\sigma}_{31}\big(\tilde{W}_1^{\mathbb{P}}(T) - \tilde{W}_1^{\mathbb{P}}(t)\big) + \tilde{\sigma}_{32}\big(\tilde{W}_2^{\mathbb{P}}(T) - \tilde{W}_2^{\mathbb{P}}(t)\big) + \tilde{\sigma}_{33}\big(\tilde{W}_3^{\mathbb{P}}(T) - \tilde{W}_3^{\mathbb{P}}(t)\big)\Bigg].\end{aligned}$$

B.1.2 Proof of Equation (3.12)

Recall from section 3.2.2 that for $t < s < T$ we have the following solution for $r_n(s)$:

$$\begin{aligned} r_n(s) &= e^{a_n(s-t)} r_n(t) + \frac{b_n - \tilde{\Sigma}_1 \tilde{\Lambda}}{a_n} \left(1 - e^{a_n(s-t)}\right) + \tilde{\sigma}_{11} \int_t^s e^{-a_n(s-u)}\, d\tilde{W}_1^{\mathbb{P}}(u) \\ &\quad + \tilde{\sigma}_{12} \int_t^s e^{-a_n(s-u)}\, d\tilde{W}_2^{\mathbb{P}}(u) + \tilde{\sigma}_{13} \int_t^s e^{-a_n(s-u)}\, d\tilde{W}_3^{\mathbb{P}}(u) \\ &= e^{a_n(s-t)} r_n(t) + \frac{b_n - \tilde{\Sigma}_1 \tilde{\Lambda}}{a_n} \left(1 - e^{a_n(s-t)}\right) + \sum_{i=1}^{3} \left[\tilde{\sigma}_{1i} \int_t^s e^{-a_n(s-u)}\, d\tilde{W}_i^{\mathbb{P}}(u) \right]. \end{aligned}$$

Integrating both sides from t to T we have:

$$\begin{aligned} \int_t^T r_n(s)\, ds = &\underbrace{\int_t^T e^{a_n(s-t)} r_n(t)\, ds}_{(1)} + \underbrace{\int_t^T \frac{b_n - \tilde{\Sigma}_1 \tilde{\Lambda}}{a_n} \left(1 - e^{a_n(s-t)}\right) ds}_{(2)} \\ &+ \sum_{i=1}^{3} \underbrace{\left[\int_t^T \tilde{\sigma}_{1i} \int_t^s e^{-a_n(s-u)}\, d\tilde{W}_i^{\mathbb{P}}(u)\, ds \right]}_{(3)}. \end{aligned}$$

Beginning with part (1) we can show:

$$\begin{aligned} \int_t^T e^{-a_n(s-t)} r_n(t)\, ds &= r_n(t) e^{a_n t} \int_t^T e^{-a_n s}\, ds \\ &= r_n(t) e^{a_n t} \left(-\frac{1}{a_n} e^{-a_n T} + \frac{1}{a_n} e^{-a_n t} \right) \\ &= r_n(t) \frac{1}{a_n} \left(1 - e^{-a_n(T-t)}\right) \\ &= r_n(t) D_n(t, T). \end{aligned}$$

Similarly, with part (2) we can show:

$$\begin{aligned} \int_t^T \frac{b_n - \tilde{\Sigma}_1 \tilde{\Lambda}}{a_n} \left(1 - e^{-a_n(s-t)}\right) ds &= \frac{b_n - \tilde{\Sigma}_1 \tilde{\Lambda}}{a_n} \left[(T-t) - \int_t^T e^{-a_n(s-t)}\, ds \right] \\ &= \frac{b_n - \tilde{\Sigma}_1 \tilde{\Lambda}}{a_n} \left[(T-t) - D_n(t, T) \right]. \end{aligned}$$

With part (3), we will need to apply the Fubini theorem (see Björk (2009)) to show:

$$\begin{aligned} \tilde{\sigma}_{1i} \int_t^T \int_t^s e^{-a_n(s-u)}\, d\tilde{W}_i^{\mathbb{P}}(u)\, ds &= \tilde{\sigma}_{1i} \int_t^T \int_u^T e^{-a_n(s-u)}\, ds\, d\tilde{W}_i^{\mathbb{P}}(u) \\ &= \tilde{\sigma}_{1i} \int_t^T D_n(u, T)\, d\tilde{W}_i^{\mathbb{P}}(u). \end{aligned}$$

Therefore, all together we have:

$$\int_t^T r_n(s)\,ds = r_n(t)D_n(t,T) + \frac{b_n - \tilde{\Sigma}_1\tilde{\Lambda}}{a_n}\big[(T-t) - D_n(t,T)\big] + \sum_{i=1}^{3}\left[\tilde{\sigma}_{1i}\int_t^T D_n(s,T)\,d\tilde{W}_i^{\mathbb{P}}(s)\right].$$

Appendix C

Chapter 4 Proofs

C.1 Estimation of Non-Filterable Parameters Proofs

C.1.1 Proof of Equation (4.6):

Since $(T-t)$ and $D_x(t,T)$ are constants, by covariance laws we can show:

$$\begin{aligned}
\hat{\rho}_{nr} = \text{Corr}\big[\Delta r_n(t), \Delta r_r(t)\big] &= \text{Corr}\left[\frac{(T-t)\Delta z_n(t,T)}{D_n(t,T)}, \frac{(T-t)\Delta z_r(t,T)}{D_r(t,T)}\right] \\
&= \frac{\text{Cov}\left[\frac{(T-t)\Delta z_n(t,T)}{D_n(t,T)}, \frac{(T-t)\Delta z_r(t,T)}{D_r(t,T)}\right]}{\sqrt{\text{Var}\left[\frac{(T-t)\Delta z_n(t,T)}{D_n(t,T)}\right]}\sqrt{\text{Var}\left[\frac{(T-t)\Delta z_r(t,T)}{D_r(t,T)}\right]}} \\
&= \frac{\frac{(T-t)^2}{D_n(t,T)D_r(t,T)}\text{Cov}\big[\Delta z_n(t,T), \Delta z_r(t,T)\big]}{\frac{(T-t)^2}{D_n(t,T)D_r(t,T)}\sqrt{\text{Var}\big[\Delta z_n(t,T)\big]}\sqrt{\text{Var}\big[\Delta z_r(t,T)\big]}} \\
&= \text{Corr}\big[\Delta z_n(t,T), \Delta z_r(t,T)\big].
\end{aligned}$$

C.1.2 Proof of Equation (4.7):

In the same way as in the proof of equation (4.6), we can show:

$$\begin{aligned}
\hat{\rho}_{nI} = \text{Corr}\left[\Delta r_n(t), \frac{\Delta I(t)}{I(t)}\right] &= \text{Corr}\left[\frac{(T-t)\Delta z_n(t,T)}{D_n(t,T)}, \frac{\Delta I(t)}{I(t)}\right] \\
&= \frac{\text{Cov}\left[\frac{(T-t)\Delta z_n(t,T)}{D_n(t,T)}, \frac{\Delta I(t)}{I(t)}\right]}{\sqrt{\text{Var}\left[\frac{(T-t)\Delta z_n(t,T)}{D_n(t,T)}\right]}\sqrt{\text{Var}\left[\frac{\Delta I(t)}{I(t)}\right]}} \\
&= \frac{\frac{(T-t)}{D_n(t,T)}\text{Cov}\left[\Delta z_n(t,T), \frac{\Delta I(t)}{I(t)}\right]}{\frac{(T-t)}{D_n(t,T)}\sqrt{\text{Var}\big[\Delta z_n(t,T)\big]}\sqrt{\text{Var}\left[\frac{\Delta I(t)}{I(t)}\right]}} \\
&= \text{Corr}\big[\Delta z_n(t,T), \frac{\Delta I(t)}{I(t)}\big].
\end{aligned}$$

C.1.3 Proof of Equation (4.8):

In the same way as in the proof of equation (4.6) and (4.7), we can show:

$$\begin{aligned}
\hat{\rho}_{rI} = \text{Corr}\left[\Delta r_r(t), \frac{\Delta I(t)}{I(t)}\right] &= \text{Corr}\left[\frac{(T-t)\Delta z_r(t,T)}{D_r(t,T)}, \frac{\Delta I(t)}{I(t)}\right] \\
&= \frac{\text{Cov}\left[\frac{(T-t)\Delta z_r(t,T)}{D_r(t,T)}, \frac{\Delta I(t)}{I(t)}\right]}{\sqrt{\text{Var}\left[\frac{(T-t)\Delta z_r(t,T)}{D_r(t,T)}\right]}\sqrt{\text{Var}\left[\frac{\Delta I(t)}{I(t)}\right]}} \\
&= \frac{\frac{(T-t)}{D_r(t,T)}\text{Cov}\left[\Delta z_r(t,T), \frac{\Delta I(t)}{I(t)}\right]}{\frac{(T-t)}{D_r(t,T)}\sqrt{\text{Var}\left[\Delta z_r(t,T)\right]}\sqrt{\text{Var}\left[\frac{\Delta I(t)}{I(t)}\right]}} \\
&= \text{Corr}\left[\Delta z_r(t,T), \frac{\Delta I(t)}{I(t)}\right].
\end{aligned}$$

C.2 Calibration Using the General Deterministic-Shift Extension Proofs

C.2.1 Proof of Equation (4.18)

Recall from equation 3.15, we simulate $I^{\mathbb{Q}}(T)|\mathcal{F}_t$ as follows:

$$\begin{aligned}
I^{\mathbb{Q}}(T) = I^{\mathbb{Q}}(t)\exp\Bigg[& -\tfrac{1}{2}\|\tilde{\Sigma}_3\|^2(T-t) \\
& + r_n^{\mathbb{Q}}(t)D_n(t,T) + \frac{b_n}{a_n}\left[(T-t) - D_n(t,T)\right] \\
& + \frac{1}{a_n}\sqrt{(T-t) - 2D_n(t,T) + \frac{1}{2}D_n(2t,2T)}\sum_{i=1}^{3}\tilde{\sigma}_{1i}\tilde{Z}_{i,t} \\
& - r_r^{\mathbb{Q}}(t)D_r(t,T) - \frac{b_r - \tilde{\Sigma}_2\cdot\tilde{\Sigma}_3}{a_r}\left[(T-t) - D_r(t,T)\right] \\
& - \frac{1}{a_r}\sqrt{(T-t) - 2D_r(t,T) + \frac{1}{2}D_r(2t,2T)}\sum_{i=1}^{3}\tilde{\sigma}_{2i}\tilde{Z}_{i,t} \\
& + \sqrt{T-t}\sum_{i=1}^{3}\tilde{\sigma}_{3i}\tilde{Z}_{i,t}\Bigg].
\end{aligned}$$

We can thus write $I^{Cal,\mathbb{Q}}(t)$ by substituting $r_n^{\mathbb{Q}}(t)$ with $r_n^{Cal,\mathbb{Q}}(t)$ and $r_r^{\mathbb{Q}}(t)$ with $r_r^{Cal,\mathbb{Q}}(t)$:

$$\begin{aligned}
I^{Cal,\mathbb{Q}}(T) = I^{Cal,\mathbb{Q}}(t) \exp\Bigg[& -\tfrac{1}{2}\|\tilde{\Sigma}_3\|^2(T-t) \\
& + r_n^{Cal,\mathbb{Q}}(t) D_n(t,T) + \frac{b_n}{a_n}\big[(T-t) - D_n(t,T)\big] \\
& + \frac{1}{a_n}\sqrt{(T-t) - 2D_n(t,T) + \frac{1}{2}D_n(2t,2T)} \sum_{i=1}^{3} \tilde{\sigma}_{1i}\tilde{Z}_{i,t} \\
& - r_r^{Cal,\mathbb{Q}}(t))D_r(t,T) - \frac{b_r - \tilde{\Sigma}_2 \cdot \tilde{\Sigma}_3}{a_r}\big[(T-t) - D_r(t,T)\big] \\
& - \frac{1}{a_r}\sqrt{(T-t) - 2D_r(t,T) + \frac{1}{2}D_r(2t,2T)} \sum_{i=1}^{3} \tilde{\sigma}_{2i}\tilde{Z}_{i,t} \\
& + \sqrt{T-t}\sum_{i=1}^{3} \tilde{\sigma}_{3i}\tilde{Z}_{i,t}\Bigg].
\end{aligned}$$

Rewriting $r_n^{Cal,\mathbb{Q}}(t) = r_n^{\mathbb{Q}}(t) + \varphi_n(t)$ and $r_r^{Cal,\mathbb{Q}}(t) = r_r^{\mathbb{Q}}(t) + \varphi_r(t)$, we can show:

$$\begin{aligned}
I^{Cal,\mathbb{Q}}(T) = I^{Cal,\mathbb{Q}}(t) \exp\Bigg[& -\tfrac{1}{2}\|\tilde{\Sigma}_3\|^2(T-t) \\
& + \Big(r_n^{\mathbb{Q}}(t) + \varphi_n(t)\Big) + \frac{b_n}{a_n}\big[(T-t) - D_n(t,T)\big] \\
& + \frac{1}{a_n}\sqrt{(T-t) - 2D_n(t,T) + \frac{1}{2}D_n(2t,2T)} \sum_{i=1}^{3} \tilde{\sigma}_{1i}\tilde{Z}_{i,t} \\
& - \Big(r_r^{\mathbb{Q}}(t) + \varphi_r(t)\Big) - \frac{b_r - \tilde{\Sigma}_2 \cdot \tilde{\Sigma}_3}{a_r}\big[(T-t) - D_r(t,T)\big] \\
& - \frac{1}{a_r}\sqrt{(T-t) - 2D_r(t,T) + \frac{1}{2}D_r(2t,2T)} \sum_{i=1}^{3} \tilde{\sigma}_{2i}\tilde{Z}_{i,t} \\
& + \sqrt{T-t}\sum_{i=1}^{3} \tilde{\sigma}_{3i}\tilde{Z}_{i,t}\Bigg].
\end{aligned}$$

Collecting terms, we arrive at equation (4.18):

$$I^{Cal,\mathbb{Q}}(T) = \frac{I^{Cal,\mathbb{Q}}(t) I^{\mathbb{Q}}(T)}{I^{\mathbb{Q}}(t)} e^{\varphi_n(t) - \varphi_r(t)},$$

which concludes the proof.